Extrathymic expression of Aire controls the induction of effective TH17 cell-mediated immune response to Candida albicans

Dobeš, Jan; Ben-Nun, Osher; Binyamin, Amit

Dobeš, J., Ben-Nun, O., Binyamin, A., Stoler-Barak, L., Oftedal, B. E., Goldfarb, Y., Kadouri, N., Gruper, Y., Givony, T., Zalayat, I., Kováčová, K., Böhmová, H., Valter, E., Shulman, Z., Filipp, D., Husebye, E. S., & Abramson, J. (2022). Extrathymic expression of Aire controls the induction of effective TH17 cell-mediated immune response to Candida albicans. Nature Immunology, 23, 1098–1108.
https://doi.org/10.1038/s41590-022-01247-6
Document Version: Accepted

Published Version: https://doi.org/10.1038/s41590-022-01247-6

Figure #	Figure title One sentence only	Filename This should be the name the file is saved as when it is uploaded to our system. Please include the file extension. i.e.: *Smith_ED_Fig1.jpg*	Figure Legend If you are citing a reference for the first time in these legends, please include all new references in the main text Methods References section, and carry on the numbering from the main References section of the paper. If your paper does not have a Methods section, include all new references at the end of the main Reference list.
Extended Data Fig. 1	Extended Data Fig. 1	EF1.pdf	**a-c)** GO enrichment analysis of upregulated differentially expressed genes from unstimulated vs. *C. albicans*- stimulated ILC3 subsets including cILC3s (related to Figure 2a) (**a**); MHCII$^+$ ILC3s (related to Figure 2b) (**b**); Aire$^+$ ILC3s (related to Figure 2c) (**c**). **d**) Heatmap of Pearson correlation according to gene expression values between individual samples analyzed in Fig. 2a-c.
Extended Data Fig. 2	Extended Data Fig. 2	EF2.pdf	**a)** Imaging flow cytometry analyzing the physical interaction between HKCA with DCs or with Aire$^+$ ILC3s. CD11c$^+$ DCs or Lineage negative cells and were isolated from mouse popliteal lymph nodes using MACS-beads depletion and then incubated with CPD-stained HKCA for 90 minutes. Samples were stained for Aire, MHCII, CD11c, Lamp1 (lysosomal marker) and DAPI and analyzed by Imaging flow cytometry. In both, Aire$^+$ ILC3 cells (Aire$^+$) and DCs (CD11c$^+$) HKCA associate with lysosomes (Lamp1). Representative images out of five independent repetitions of the experiment are shown. (**b)** Comparison of the capacity of different immune subsets (B cells, Ly6C$^+$ MNPs, CD11b$^+$ MNPs, CD11c$^+$ MNPs and Aire$^+$ ILC3s) to endocytose CPD-labeled HKCA in an in-vitro endocytosis assay. Subsets were FACS-sorted and incubated with HKCA-CPD for three hours. The frequency of cells that have successfully internalized HKCA-CPD was then assessed by flow cytometry (mean ± SD; n=3). **c-d**) Comparison of the capacity of either wild-type or Galectin-3/Dectin-1-double knockout (dKO) Aire+ ILC3s (c) or DCs (d) to endocytose CPD-labeled HKCA at 37°C or at 4°C. Corresponding populations were isolated from WT or dKO mice and kept either at 37°C or at 4°C. The internalization of HKCA-CPD by the cells was measured by FACS (mean ± SD; n=3). **e)** Representative gating

			strategy of APC populations related to Fig. 3c-g. **f)** FACS analysis of in vitro assay related to Fig. 3c. **g)** Graphical summary of an experimental setting relevant for data shown in h. Wild-type mice were intravenously stimulated HKCA in specified timepoints and APC population were isolated using gating strategy depicted in e. **h)** FACS analysis of in vitro assay related to Fig. 3d-f assessing the antigen presentation of the corresponding cell subsets.
Extended Data Fig. 3	Extended Data Fig. 3	EF3.pdf	**a)** FACS analysis validating that Aire protein expression in the entire LN-resident cell compartment is exclusively restricted to a CD45 positive, lineage negative (Lin 1: TCR-β, CD19, Gr-1, F4/80, CD11b, CD11c, NK1.1; Lin 2: CD3, B220), NKp46-negative, MHCII positive, Rorγt positive cell subset – previously identified as Aire^{+} ILC3s. **b)** Back-gating FACS analysis of Aire-expressing cells identified in a. **c)** Representative flow cytometry dot plots showing the frequencies of transferred CD45.1^{+} OT-II T cell (red gate) vs. CD45.1/CD45.2 double positive control T cell (blue gate) populations 2 days after the transfer. **d)** Statistical analysis of ratios related to b (n=5 per group, mean ± SD, two-tailed Student´s t-test) of OT-II vs. control T two days after the transfer. **e-f**) Survival curves of WT (Aire$^{+/+}$) and knockout (Aire$^{-/-}$) mice (n≥10 mice per group) on either on NOD **(e)** and C57Bl/l **(f)** genetic background after systemic challenge with live *C. albicans*. Mice were *i.v.* injected every second day by heat-killed *C. albicans* (HKCA) for the duration of three weeks. Subsequently, mice were infected by alive *C. albicans* and monitored for survival. Long-rank (Mantel-Cox) test was used to calculate the indicated p-value. **g-h)** Quantitative PCR analysis assessing the presence of *C. albicans*-specific DNA in the liver (g) and small intestine (h) from *Rorc*-Cre^{-} Aire$^{fl/fl}$ (WT) and *Rorc*-Cre^{+}Aire$^{fl/fl}$ (ILC3$^{\Delta Aire}$) mice (n=6, mean ± SD, two-tailed Student´s t-test). **i-j)** ELISA assessing the amount of IL-17 **(i)** or (IL-22) **(j)** autoantibodies in the sera of 8-week old untreated Aire$^{+/+}$ vs. Aire$^{-/-}$ mice on NOD and C57Bl/6 (B6) genetic background (n=6 per group, two-tailed Student´s t-test). Data are shown as mean of optical density ± SD. Data are

			shown as mean of optical density ± SD. P-value indicators: *** = p-value < 0.0001, ** = p-value < 0.001, * = p-value < 0.05, ns = not significant.
Extended Data Fig. 4	Extended Data Fig. 4	EF4.pdf	**a)** Experimental outline relevant to data shown in Fig 6a, b: Wild-type mice were orally colonized by *C. albicans* and analyzed in indicated time points. **b)** Representative FACS gating strategy of Als1-tet^{+} T cells. **c)** Experimental outline relevant to data shown in **(d)** and **(e)**: WT **(**Aire$^{+/+}$) and Aire$^{-/-}$ were orally colonized by *C. albicans* and analyzed after two weeks. **d)** Representative FACS plot of Als1-tet^{+} T cells. Cells were isolated from pLNs and spleens of mice described in **(c)**. Counts of Als1-tet^{+} cells are highlighted in red rectangles (left panel). Statistical analysis of the same representative experiment showing the total counts (mean ± SD, two-tailed Student´s t-test, n=6). Representative experiment is shown. **e)** Quantitative PCR analysis assessing the presence of *C. albicans*-specific DNA in the ileal part of small intestine from WT and Aire-deficient mice (n=5, mean ± SD, two-tailed Student´s t-test). **f)** Experimental outline relevant to data shown in **(g)** and **(h)**. Bone-marrow (BM) chimeras restricting Aire expression either to hematopoietic (Aire$^{+/+}$ BM → Aire$^{-/-}$) or stromal compartment (Aire$^{-/-}$ BM → Aire$^{+/+}$) were generated by reciprocal BM transfer to recipient mice after 900 rad whole-body irradiation. Six weeks after the BM transfer, the mice were orally colonized by *C. albicans* and analyzed after two weeks. **g)** Representative FACS plot of Als1-tet^{+} T cells. Counts of Als1-tet^{+} cells are highlighted in red rectangles (left panel). Statistical analysis of the same representative experiment showing the total counts (n=6, mean ± SD, two-tailed Student´s t-test). Representative experiment is shown. **h)** Quantitative PCR analysis assessing the presence of *C. albicans*-specific DNA in the ileal part of small intestine from reciprocal bone-marrow chimeras (n=6, mean ± SD, two-tailed Student´s t-test). **i)** Experimental outline relevant to data shown in j and k. CD90-disperate chimeras were created by adoptive transfer of T cells and B-lymphocytes from CD90.1 mice to Rag1$^{-/-}$ (CD90.2) recipients and let to proliferate for 2 months. Mice were treated by anti-CD90.2 or isotype

			control antibody prior the *C. albicans* oral colonization and then each third day and analyzed after two weeks. **j)** Representative FACS plot of Als1-tet^{+} T cells. Counts of tetramer positive cells are highlighted in red rectangles (left panel). Statistical analysis of the same representative experiment showing the total counts (n=6, mean ± SD, two-tailed Student´s t-test). Representative experiment is shown. **k)** Quantitative PCR analysis assessing the presence of *C. albicans*-specific DNA in the ileal part of small intestine from CD90-disparate chimeras (n=6, mean ± SD, two-tailed Student´s t-test). P-value indicators: *** = p-value < 0.0001, ** = p-value < 0.001, * = p-value < 0.05, ns = not significant.
Extended Data Fig. 5	Extended Data Fig. 5	EF5.pdf	**a-e**) Flow cytometry analysis of *C albicans*-specific T cells (using Als1-tet) after oral colonization. Aire whole-body knockout mice (Aire$^{-/-}$), their wild-type littermates (Aire$^{+/+}$), WT **(***Rorc*-Cre^{-}Aire$^{fl/fl}$) and ILC3$^{\Delta Aire}$ (*Rorc*-Cre^{+}Aire$^{fl/fl}$) were orally colonized by *C. albicans* and analyzed after 24 hours (left panel) or two weeks (right panel). **a)** Representative FACS plot of Als1-tet^{+} T cells. Cells were isolated from pLNs and spleens (SLO), oral mucosa, esophagus and intestine of mice described above 24 hours (left panel) or 2 weeks (right panel) post *C. albicans* colonization. Counts of Als1-tet^{+} cells are highlighted in red rectangles. **b-e)** Statistical analysis of the Als1-tetramer counts (n=6, mean ± SD, two-tailed Student´s t-test in SLO (b), oral mucosa (c), esophagus (d) and small intestine (e) 24 hours (left panel) or 2 weeks (right panel) post *C. albicans* colonization (n=6, mean ± SD, two-tailed Student´s t-test). P-value indicators: *** = p-value < 0.0001, ** = p-value < 0.001, * = p-value < 0.05, ns = not significant.
Extended Data Fig. 6	Extended Data Fig. 6	EF6.pdf	**a)** Representative FACS gating strategy of Roryt^{+} CD4^{+} TCR-β^{+} T$_{H}$17 cells in pLNs two weeks after *C. albicans* colonization of *Rorc*-Cre^{-} Aire$^{fl/fl}$ (WT) and *Rorc*-Cre^{+}Aire$^{fl/fl}$ (ILC3$^{\Delta Aire}$) mice. **b)** Statistical analysis of related to a). The plot is showing the frequency from parent gate (n=6, mean ± SD, two-tailed Student´s t-test). **c)** Representative FACS gating strategy of Roryt^{+} CD4^{+} TCR-β^{+} T$_{H}$17 cells in mesenteric lymph nodes (mLN) two weeks after *C. albicans*

			colonization of *Rorc*-Cre^{-} Aire$^{fl/fl}$ (WT) and *Rorc*-Cre^{+}Aire$^{fl/fl}$ (ILC3$^{\Delta Aire}$) mice. **d)** Statistical analysis of related to c). The plot is showing the frequency from parent gate (n=6, mean ± SD, two-tailed Student´s t-test). **e)** Representative FACS gating strategy of Roryt^{+} CD4^{+} TCR-β^{+} T_H17 cells in lamina propria two weeks after *C. albicans* colonization of *Rorc*-Cre^{-} Aire$^{fl/fl}$ (WT) and *Rorc*-Cre^{+}Aire$^{fl/fl}$ (ILC3$^{\Delta Aire}$) mice. **f)** Statistical analysis of related to e). The plot is showing the frequency from parent gate (n=6, mean ± SD, two-tailed Student´s t-test). P-value indicators: *** = p-value < 0.0001, ** = p-value < 0.001, * = p-value < 0.05, ns = not significant.
Extended Data Fig. 7	Extended Data Fig. 7	EF7.pdf	**a-d)** Colony forming units (CFU)-based assay determining the overgrowth of *C albicans* 1 day (left panel) and 14 days (right panel) after the oral colonization. The tissues were isolated from Aire whole-body knockout mice (Aire$^{-/-}$), their wild-type littermates (Aire$^{+/+}$), *Rorc*-Cre^{-} Aire$^{fl/fl}$ (WT) and *Rorc*-Cre^{+}Aire$^{fl/fl}$ (ILC3$^{\Delta Aire}$) mice. CFU was determined by plating the lysates obtained from the kidney (a), oral cavity (b), esophagus (c), small intestine (d) (n=6, mean ± SD, two-tailed Student´s t-test). P-value indicators: *** = p-value < 0.0001, ** = p-value < 0.001, * = p-value < 0.05, ns = not significant.
Extended Data Fig. 8	Extended Data Fig. 8	EF8.pdf	**a)** Experimental outline relevant to data shown in **(b-d)**. *Rorc*-Cre^{-} Aire$^{fl/fl}$ (WT) and *Rorc*-Cre^{+}Aire$^{fl/fl}$ (ILC3$^{\Delta Aire}$) were first primed by repeated injections of heat-killed *C. albicans* (HKCA) for two weeks, then exposed to prolonged protocol of oropharyngeal candidiasis and analyzed five days later. **b)** Representative FACS plot of Als1-tet^{+} T cells . Cells were isolated from pLNs and spleens of mice described in a). Counts of Als1-tet^{+} cells are highlighted in red rectangles (left panel). Statistical analysis of the same representative experiment showing the total counts of Als1-tet^{+} cells (n=6, mean ± SD, two-tailed Student´s t-test). Representative experiment is shown. **c)** Representative FACS plot of Als1-tet^{+} T cells. Cells were isolated from tongue mucosae of mice described in a). Counts of Als1-tet^{+} cells are highlighted in red rectangles (left panel). Statistical analysis of the same representative experiment showing

			the total counts of Als1-tet^{+} cells (n=6, mean ± SD, two-tailed Student´s t-test). Representative experiment is shown.
Extended Data Fig. 9	Extended Data Fig. 9	EF9.pdf	**a)** Representative FACS-sorting strategy of Aire^{+} ILC3s from reporterAire-GFP positive mice. The plots are showing the frequency from parent gates. Lineage: CD3, CD19, CD11c, CD11b, N.K.1, F4/80, Gr1, B220. **b)** Back-gating of Aire-GFP^{+} cells.
Extended Data Fig. 10	Extended Data Fig. 10	EF10.pdf	**a)** Experimental outline relevant to data shown in **(b-c)**. WT (*Rorc*-Cre^{-}Aire$^{fl/fl}$) and ILC3$^{\Delta Aire}$ (*Rorc*-Cre^{+}Aire$^{fl/fl}$) mice were transferred with naïve OT-II CD4^{+} T cells and subsequently injected with HKCA-OVA four times during a single week. **b)** Statistical analysis of the frequencies of OT-II T-cells subtypes (n=4, mean ± SD, two-tailed Student´s t-test). **c**) GO enrichment analysis of upregulated differentially expressed genes from *Rorc*-GFP^{+} OT-II T cells vs Non-proliferating OT-II T cells comparison. **d)** Graphical model summarizing the role of Aire^{+}ILC3s in the induction of Candida-specific T_H17 response. While the immediate immune response to *C. albicans* infection is dominated by neutrophils, monocytes and macrophages, Aire^{+}ILC3s become essential in the later phase, as they facilitate clonal expansion of the primed T_H17 cell clones in the LN. The expanded candida-specific T_H17 clones subsequently limit *C. albicans* overgrowth at mucosal surfaces and its dissemination into epithelial tissues; **e)** Scheme illustrating the putative mechanism through which Aire^{+} ILC3 cells induce the expansion of candida-specific T_H17 clones.

1

Item	Present?	Filename This should be the name the file is saved as when it is uploaded to our system, and should include the file extension. The extension must be .pdf	A brief, numerical description of file contents. i.e.: *Supplementary Figures 1-4, Supplementary Discussion, and Supplementary Tables 1-4.*

Supplementary Information	Yes	Suppl-table.pdf	Supplementary Table 1-2
Reporting Summary	Yes	NI-A28785I reporting summary.pdf	
Peer Review Information	No	*OFFICE USE ONLY*	

Extrathymic expression of Aire controls the induction of effective T_H17 cell-mediated immune response to *Candida albicans*

Jan Dobeš[1,2], Osher Ben-Nun[1], Amit Binyamin[1], Liat Stoler-Barak[1], Bergithe E. Oftedal[3,4], Yael Goldfarb[1], Noam Kadouri[1], Yael Gruper[1], Tal Givony[1], Itay Zalayat[1], Katarína Kováčová[2], Helena Böhmová[2], Evgeny Valter[2], Ziv Shulman[1], Dominik Filipp[5], Eystein S. Husebye[3,4] & Jakub Abramson[1]

[1] Department of Immunology, Weizmann Institute of Science, Rehovot, Israel

[2] Department of Cell Biology, Faculty of Science, Charles University, Prague, Czech Republic

[3] Department of Clinical Science, University of Bergen, Bergen, Norway

[4] Department of Medicine, Haukeland University Hospital, Bergen, Norway

[5] Laboratory of Immunobiology, Institute of Molecular Genetics of the Czech Academy of Sciences, Prague, Czech Republic

Corresponding author:

Prof. Jakub Abramson
Department of Immunology
Weizmann Institute of Science
Herzl St. 234
76100 Rehovot,
Israel
Mail: jakub.abramson@weizmann.ac.il
Telephone: +972-8-934-2776

ABSTRACT

Patients with loss of function in the gene encoding the master regulator of central tolerance *AIRE* suffer from a devastating disorder called autoimmune polyendocrine syndrome type 1 (APS-1), characterized by a spectrum of autoimmune diseases and severe mucocutaneous candidiasis. While the key mechanisms underlying the development of autoimmunity in APS-1 patients are well-established, the underlying cause for the increased susceptibility to *Candida albicans* infection remains less understood. Here we show that Aire^{+}MHCII^{+} type-3 innate lymphoid cells (ILC3) could sense, internalize and present *Candida albicans*, and had a critical role in the induction of candida-specific T_H17 cell clones. Extrathymic *Rorc*-Cre-mediated deletion of *Aire* resulted in impaired generation of candida-specific T_H17 cells and subsequent overgrowth of *C. albicans* in the mucosal tissues. Collectively, our observations identify a previously uncharacterized regulatory mechanism for effective defense responses against fungal infections.

The transcriptional regulator Aire has an essential role in the induction of self-tolerant T cells during thymic development by controlling the expression of thousands of self-antigen genes in medullary thymic epithelial cells (mTECs)[1, 2]. Presentation of self-antigens by mTECs is essential for the deletion of self-reactive T cell clones[3] or their conversion into regulatory T cells (T_{reg} cells) [4, 5]. *Aire* deficiency results in impaired T_{reg} cell generation and escape of self-reactive T cells into the periphery, leading to breakdown of immunological tolerance to various parenchymal tissues[1].

Patients with *AIRE* deficiency develop a rare genetic disorder called autoimmune polyendocrine syndrome type-1 (APS-1; also known as autoimmune polyendocrinopathy candidiasis ectodermal dystrophy – APECED, OMIM: 240300), which is characterized by autoimmune pathologies such as hypoparathyroidism and primary adrenocortical insufficiency (Addison's disease), with additional autoimmune disorders such as hypothyroidism, type-1 diabetes, premature ovarian failure, pernicious anemia, vitiligo, alopecia, keratitis or intestinal malabsorption occurring with lower frequency [6, 7]. In addition, the vast majority (75-100%) of APS-1 patients develop chronic mucocutaneous candidiasis (CMC), mainly characterized by *C. albicans* overgrowth in the oral cavity, esophagus and nails as early as 1 year of age (median 5 years) [8, 9]. Because candidiasis is a common complication in people born with a loss of function mutation in various genes linked to the $CD4^+$ helper type 17 (T_H17 cell)-mediated response (e.g. *RORC*[10], *IL17F*[11], *STAT3*[12], *CLEC7A*[13], *CARD9*[14] or *STAT1*[15]), T_H17 cells are assumed to have an indispensable role in long term protection against *C. albicans* infection[16]. APS-1 patients have been reported to develop autoantibodies against the T_H17 effector cytokines IL-17A, IL17-F and/or IL-22[17, 18], suggesting that the increased susceptibility to *C. albicans* might also be caused by an autoimmune-mediated mechanism. However, a considerable fraction of APS-1 patients with very low or no IL-17 or IL-22 autoantibodies still develop CMC[17, 18], indicating the correlation between the IL-17- and/or IL-22-specific autoantibodies and candidiasis is incomplete and that additional mechanism(s) may be involved.

In addition to its well-established expression pattern in the thymus, Aire was reported to be expressed in a rare population of cells residing in the lymph nodes (LNs) and bearing the hallmarks of a subset of MHCII$^+$ type-3 innate lymphoid cells (ILC3)[19]. Considering that these Aire$^+$ MHCII$^+$ ILC3 (hereafter Aire$^+$ ILC3s) also express the molecular machinery for antigen presentation and T cell activation (MHCII, CD80, CD86, ICOSL)[19], we investigated whether extrathymic expression of *Aire* in this ILC3 subset may contribute to the adaptive immune response to *C. albicans*. Here we show that Aire$^+$ ILC3 cells sensed and internalized *C. albicans*, and effectively presented *C. albicans* epitopes on their MHCII. Moreover, extrathymic (but not thymus-specific) ablation of Aire impaired the expansion of the candida-specific T_H17 cell pool and resulted in overgrowth of *C. albicans* at various mucosal surfaces.

RESULTS

Aire$^+$ ILC3s express receptors involved in *C. albicans* sensing

To test whether peripheral expression of Aire in ILC3s was required for the induction or modulation of an effective immune response to *C. albicans* infection, we determined whether ILC3s in general and Aire$^+$ ILC3s in particular expressed pattern recognition receptors (PRRs) for *C. albicans*. We used *Rorc*-Cre$^+$flox-STOP-flox-tdTomato reporter mice that were crossed with *Aire*-GFP$^+$ transgenic reporter mice (hereafter *Rorc*^{Tomato} *Aire*^{GFP} mice), in which the tdTomato reporter is expressed in all cells with a history of *Rorc* expression and the green fluorescent protein (GFP) is expressed in cells with an active *Aire* locus. ILC3s isolated from the popliteal lymph node (pLN) by flow cytometry-based sorting as lineage$^-$(CD3, TCR-β, CD45RB, CD19, Gr1, F4/80, CD11b, CD11c) *Rorc*-tdTomato$^+$ cells were divided according to their MHCII and *Aire*-GFP expression into MHCII$^-$*Aire*-GFP$^-$ conventional ILC3s (hereafter cILC3s), MHCII$^+$*Aire*-GFP$^-$ ILC3s (hereafter MHCII$^+$ ILC3s) and MHCII$^+$*Aire*-GFP$^+$ ILC3s (hereafter Aire$^+$ ILC3s) (Fig. 1a). In addition, to compare the molecular characteristics of these three ILC3 subsets with conventional antigen presenting cells (APCs) that can sense *C. albicans*[20], we isolated CD11c$^+$CD11b$^+$ MHCII$^+$ dendritic cells (DCs) from the *Rorc*^{Tomato} *Aire*^{GFP} mice. All sorted populations were analysed by bulk RNA sequencing. Clustering analysis highlighted relatively large transcriptional similarity between all cell subsets expressing MHCII (i.e. MHCII$^+$ ILC3, Aire$^+$ ILC3 and DC), and in particular between the Aire$^+$ ILC3s and MHCII$^+$ ILC3s (Fig. 1b). All three ILC3 subsets were, as expected, characterised by low expression of genes specific for hematopoietic stem cells (*Cd34, Slamf1*), T cells (*Cd4, Cd8, Foxp3)*; B cells (*Cd19, Cd79a)*; granulocytes (*Ly6c1, Ly6g5b, Siglecf)*; macrophages and monocytes (*Itgam, Siglech)*; dendritic cells (*Itgax, Csf1r, Cd207*) and had high expression of genes associated with ILC3s (*Rorc, Il1r1, Il7r, Kit, Ccr6*) (Fig. 1c). Unlike cILC3s, MHCII$^+$ ILC3 and the Aire$^+$ ILC3s had high expression of genes encoding MHCII (*H2-Aa, H2-Ab1*) (Fig. 1d), while Aire$^+$ ILC3s also had high expression of *Aire* and genes encoding

costimulatory molecules (*Cd80, Cd86*) at levels comparable to DCs (Fig. 1d). The Aire^{+} ILC3s also expressed transcripts for several key PRRs implicated in sensing *C. albicans*, such as *Tlr2*[21, 22], dectin-1 (*Clec7a*)[23, 24] or galectin-3 (*Lgals3*)[25, 26] (Fig. 1e) and signaling molecules downstream of these receptors (*Myd88, Syk*) (Fig. 1f). The protein expression of the *C. albicans*-sensing receptors including dectin-1, galectin-3 and Tlr2 on Aire^{+} ILC3s was confirmed by flow cytometry in steady-state conditions and was comparable to the expression on these receptors on DCs (Fig. 1g). These results collectively suggested that Aire^{+} ILC3s expressed genes implicated in antigen presentation, T cell activation[19] and also *C. albicans* sensing.

C. albicans induces transcriptional changes in ILC3 subsets

To test whether *C. albicans* could induce the activation of ILC3s in general, and Aire^{+} ILC3s in particular, we performed bulk RNA sequencing of Aire^{+} ILC3s, MHCII^{+} ILC3s and cILC3s sorted from pLN of *Rorc*^{Tomato} *Aire*^{GFP} mice that were intravenously injected at 1 day intervals for 3 days with heat-killed *Candida albicans* (HKCA) or PBS and analyzed 24 hours after the last injection. All three ILC3 subsets, and particularly the Aire^{+} ILC3s subset isolated from HKCA-challenged mice showed transcriptional changes compared to PBS-challenged controls (Fig. 2a-c). cILC3s from HKCA-challenged mice significantly upregulated 149 genes (Fc≥2.0, adjusted p-value≤0.05) compared to PBS-treated controls (Fig. 2a), with genes encoding several PRR implicated in *C. albicans*-sensing (*Lgals3, Clec7a, Clec4d, Clec4e and Cd209b*) or molecules involved in antigen presentation (*H2-Aa, H2-Ab1, H2-Eb1 and Cd74*), co-stimulation (*Cd86)* or induction of pro-inflammatory response (*Il1a, Il1b and 1l18*) among the most upregulated (Fig. 2a, Extended Data Fig. 1a). This suggested that cILC3s may upregulate *Candida*-sensing receptors and/or MHCII molecules in response to the inflammatory conditions engendered by *C. albicans* stimulation. MHCII^{+} ILC3s from the HKCA-challenged mice significantly induced the expression of 641 genes, including *Aire*, which was the most significantly upregulated gene (p-value≤1×10^{-23}; FC>7)

compared to their PBS-their counterparts, and further upregulated the expression of *Clec7a* (dectin-1), *H2-Ab1* (MHCII) and *Cd86*, while downregulating the expression of several key ILC3-specific genes, such as *Il17a*, *Il17f* and *Il12rb1* (Fig. 2b, Extended data Fig. 1b). These observations suggested that the HKCA challenge potentiated the antigen presentation capacity of the MHCII$^+$ ILC3 subset, while limiting their effector functions as IL-17-producing cells (Fig. 2b, Extended Data Fig. 1b). Moreover, fold-change/fold-change analysis comparing MHCII$^+$ ILC3s from HKCA-stimulated vs. PBS-stimulated mice and Aire$^+$ ILC3 vs. MHCII$^+$ ILC3s from PBS-treated mice showed that MHCII$^+$ ILC3s from HKCA-treated mice acquired a transcriptional signature similar to that of Aire$^+$ ILC3s (Fig. 2d). This suggested that exposure of MHCII$^+$ ILC3s to HKCA could likely initiate the acquisition of a transcriptional signature characteristic of Aire$^+$ ILC3s (Fig. 2d, e, Extended Data Fig. 1d).

Finally, Aire$^+$ ILC3s from HKCA-stimulated mice significantly upregulated 777 genes compared to PBS-treated mice, including cytokines or cytokine receptors (*Il6*, *Bmp2*, *Il7r*, *Il23r*, *Il2rb*), chemokines (*Ccl2*), *C. albicans*-sensing receptors (*Clec7a*), cell adhesion molecules (*Vcam1*, *Cadm1*), co-stimulatory molecules (*Cd86*) and enzymes involved in proinflammatory response (*Ptgs2*) (Fig 2c). Moreover, the HKCA challenge lead to a significant upregulation of *Il6*, which along with TGF-β, induces the polarization of naïve T cells to the T_H17 subset and their clonal expansion [27, 28, 29] (Fig. 2c, Extended Data Fig. 1c). These results indicated that *HKCA* induced distinct transcriptional programs in the three ILC3 subsets analyzed, including the upregulation of genes involved in antigen presentation, co-stimulation and candida sensing in cILC3s and MHCII$^+$ ILC3s, the upregulation of *Aire* in MHCII$^+$ ILC3s and the upregulation of *Il6* in the Aire$^+$ ILC3s, suggesting that Aire$^+$ ILC3s could play a role in the induction or regulation of the adaptive immune response to *C. albicans*.

Aire$^+$ ILC3s internalize *C. albicans* for antigen presentation

Next, we investigated whether Aire$^+$ ILC3s could uptake *C. albicans* by endocytosis. To this end, we performed imaging flow cytometry (Imagestream) analysis of MACS-enriched lineage negative (Lin^{neg}: CD3$^-$, TCR-β$^-$, CD45RB$^-$, CD19$^-$, Gr1$^-$, F4/80$^-$, CD11b$^-$, CD11c$^-$) cell fraction or CD11c$^+$DCs isolated from pLN and incubated ex-vivo with cell proliferation dye (CPD)-stained HKCA (HKCA-CPD). After 30 minutes of co-incubation, most Aire$^+$ ILC3s were physically associated with HKCA-CPD (Fig. 3a), whether through cell-cell interactions or internalization of the HKCA-CPD into their cytoplasm. After 90 minutes of co-incubation, most Aire$^+$ ILC3s had intracellular CPD signals (Fig. 3b), suggesting ingestion of HKCA-CPD. Vesicles containing internalized fungi fused with the lysosomes in both Aire$^+$ ILC3s and DCs (Extended Data Fig. 2a), suggesting that Aire$^+$ ILC3s had endocytic capacity for *C. albicans*. Moreover, while the capacity of Aire$^+$ ILC3s to endocytose HKCA-CPD was comparable to CD11c$^+$ or CD11b$^+$ mononuclear phagocytes (MNPs) (Extended Data Fig. 2b), the endocytic capacity of both MHCII$^+$ ILC3s and cILC3s was substantially lower than that of Aire$^+$ ILC3s (Extended Data Fig. 2b). Moreover, similarly to DCs, the endocytic capacity of Aire$^+$ ILC3s cells was partially dependent on the expression of dectin-1 and galectin-3 and was reduced at 4°C (Extended Data Figure 2c, d).

To assess the capacity of Aire$^+$ ILC3s to present candida-derived antigens under *in vitro* conditions, we FACS-sorted pLN-resident Aire$^+$ ILC3s and other types of APCs (B cells, Ly6C$^+$ MNPs, CD11b$^+$ MNPs, CD11c$^+$ MNPs) from Balb/c wild-type mice using a gating strategy described in Extended Data Fig. 2e), stimulated them with HKCA or transgenic HKCA expressing OVA (HKCA-OVA) and incubated them for 17 hours with an NFAT-GFP DO11.10 TCR reporter cell line[4], which turn on GFP expression in response to TCR stimulation by OVA$^{323-339}$ peptide presented in the context MHCII molecules. Based on this *in vitro* assay, CD11b$^+$ MNPs were the most efficient APCs (Fig. 3c), while CD19$^+$ B cells and Ly6C$^+$ MNPs showed negligible antigen presentation capacity (Fig 3c). The Aire$^+$ ILC3s showed substantial capacity to present HKCA-

derived antigens, comparable to that of CD11c$^+$ MNPs and ~5-fold lower than that of CD11b$^+$ MNPs (Fig. 3c; Extended Data Fig. 2f).

To assess the capacity of Aire$^+$ ILC3s to present candida-derived antigens under more physiological conditions, we sorted Aire$^+$ ILC3s and other types of APCs (B cells, Ly6C$^+$ MNPs, CD11b$^+$ MNPs, CD11c$^+$ MNPs) from the pLNs of Balb/c wild type mice injected with either HKCA-OVA or HKCA at 12, 24 or 72 hours before sorting (Extended Data Fig. 2g). The sorted cells were then co-incubated with the NFAT-GFP DO11.10 TCR reporter cells line for 17 hours and their antigen presentation capacity was determined by the frequency of cells expressing the NFAT-GFP reporter. CD11b$^+$ MNPs isolated 12 hours after the HKCA challenge showed the highest antigen presentation capacity, as measured by the frequency of NFAT-GFP$^+$ cells (~1.7%) (Fig. 3d, Extended Data Fig. 2h). Their capacity to induce the NFAT-GFP signal declined at 24 hours (Fig. 3e, Extended Data Fig. 3d) and largely diminished at 72 hours after the HKCA challenge (Fig. 3f, Extended Data Fig. 2h). Both, Aire$^+$ ILC3s and CD11c$^+$ MNPs induced the highest frequency of NFAT-GFP$^+$ cells (1.2% and 0.7 % respectively) at 72 hours after the HKCA challenge (Fig. 3f, Extended Data Fig. 2h). These data suggested that while CD11b$^+$ MNPs dominated the early antigen-presentation phase, Aire$^+$ ILC3s were more efficient at presenting candida-derived antigens at later timepoints.

To examine the capacity of Aire$^+$ ILC3s to present *C. albicans*-derived antigens to T cells in the pLNs, we performed *ex vivo* two-photon imaging in *Aire*-GFP reporter mice that were adoptively transferred with OT-II T cells bearing OVA-specific TCR and endogenously expressing tdTomato fluorescence protein (OT-II^{tdTomato}). The mice were intravenously stimulated either with HKCA-OVA or HKCA as control, and two-photon excitation microscopy on explanted pLNs was used to visualize the interactions between *Aire*-GFP$^+$ cells and OVA-specific OT-II^{tdTomato} T cells (Fig. 3g). While we did not observe any physical interaction between *Aire*-GFP$^+$ cells and OT-II^{tdTomato} T cells in pLNs isolated from mice stimulated with HKCA, we observed numerous such interactions in pLNs isolated from mice stimulated by HKCA-OVA (Fig. 3g). These observations suggested that

Aire^{+} ILC3s might present candida-derived antigens to T cells and that they could exert this function at later timepoints compared to conventional APCs.

Aire^{+} ILC3s are required for induction of candida-specific T_H17

To determine whether Aire^{+} ILC3s, and, in particular, the expression of *Aire* in these cells regulated the adaptive immune response to *C. albicans*, we aimed to conditionally inactivate Aire in Aire^{+} ILC3s. To this end, we generated *Rorc*-Cre^{+}*Aire*$^{fl/fl}$ (hereafter ILC3$^{\Delta Aire}$) [30, 31], in which Aire is ablated in all cells that either actively express *Rorc* or have *Rorc* expression history. Because the expression of Aire in the pLNs of wild-type mice was restricted to Lin^{neg}Rorγt^{+}MHCII^{+} cells[19] (Extended Data Fig. 3a, b), this strategy allowed us to specifically inactivate Aire expression in Aire^{+} ILC3s. As controls, we generated *Foxn1*-Cre *Aire*$^{fl/fl}$ mice (hereafter TEC$^{\Delta Aire}$), in which Aire is deleted in thymic epithelial cells (TEC). Using flow cytometry, we could not detect any Aire protein expression in samples prepared from the pLN of ILC3$^{\Delta Aire}$ mice, while Aire protein was detected in the ILC3$^{\Delta Aire}$ thymus samples (Fig. 4a). Conversely, Aire protein was detected in the pLNs, but not the thymus, of TEC$^{\Delta Aire}$ mice (Fig. 4a). We next intravenously transferred naïve OT-II T cells from CD45.1 expressing GFP fluorescent protein under the *Rorc*-promoter (OT-II-*Rorc*-GFP) equally mixed with control polyclonal T cells from CD45.1/CD45.2 wild-type mice into CD45.2 positive wild-type or ILC3$^{\Delta Aire}$ mice, followed by stimulation of recipient mice with HKCA-OVA or HKCA as control in consecutive 2 days intervals and analyzed 2 or 14 days after the first injection. While no significant differences in OT-II-*Rorc*-GFP T cell cellularity and/or proliferation were observed at day 2 post-transfer between the HKCA-OVA or HKCA-stimulated wild-type vs. ILC3$^{\Delta Aire}$ mice (Extended Data Fig. 3 c,d), the OT-II-*Rorc*-GFP T cells transferred in the HKCA-OVA-stimulated wild-type mice showed a ~2.5 fold proliferative expansion at day 14 post-transfer compared to the HKCA-OVA-stimulated ILC3$^{\Delta Aire}$ mice (Fig. 4b, c). The frequency

of CD45.1^{+} OT-II T cells in the HKCA-OVA-treated ILC3$^{\Delta Aire}$ mice was decreased by > 8-fold compared to HKCA-OVA-treated wild-type controls (Fig. 4b, c). Moreover, approximately 10% of the CD45.1^{+} OT-II T cells transferred in the HKCA-OVA-stimulated wild-type mice differentiated into *Rorc*-GFP^{+} T_H17 cells (Fig. 4d). In contrast, the frequency (Fig. 4d) and number (Fig. 4e) of CD45.1^{+} *Rorc*-GFP^{+} OT-II T_H17 cells in HKCA-OVA-treated ILC3$^{\Delta Aire}$ was reduced by ~20 fold and ~100-fold, respectively, compared to HKCA-OVA-treated wild-type controls at day 14 post-transfer, suggesting that *Aire* expression in ILC3s was required for the induction of effector T_H17 cells in response to *C. albicans* stimulation.

Next, we performed MHCII tetramer staining for *C. albicans*-specific epitopes derived from the agglutinin-like protein 1 (Als1). Specifically, pooled spleen or pLN-resident CD4^{+} T cells isolated from ILC3$^{\Delta Aire}$, TEC$^{\Delta Aire}$ or their wild-type littermates that had been stimulated with HKCA for two weeks prior to isolation were stained with Als1-specific tetramers (Als1-Tet) and analyzed by flow cytometry. We observed a significant reduction in the number of Als1-Tet^{+}CD44^{+}CD4^{+} activated T cells isolated from the spleen and pLNs of ILC3$^{\Delta Aire}$ mice compared to wild-type or TEC$^{\Delta Aire}$ mice (Fig 4f, g), suggesting that extrathymic, but not thymic expression of Aire was critical for the induction of candida-specific T cells.

To investigate whether a similar defect of T cell response to candida was found in APS-1 patients, we stimulated the peripheral blood mononuclear cell (PBMC) fraction from APS-1 patients or healthy individuals with HKCA and monitored T cell proliferation four days later. We observed a significant decrease (~3-fold) in both the frequency of HKCA-induced RorγT^{+} T_H17 cells (Fig. 4h, i), as well as in the amount of IL-17A released in supernatants from PBMCs isolated from APS-1 vs. healthy controls (Fig. 4j). Collectively, these data suggest that expression of Aire in ILC3s was required for the expansion of candida-specific CD4^{+} Rorγt^{+} T cell clones.

Extrathymic Aire is critical for effective response to *C. albicans*

Next, we sought to determine whether loss of Aire expression in ILC3s could impair the clearance of live *C. albicans in vivo*. Because *C. albicans* is generally completely absent in mice housed under specific pathogen free (SPF) conditions[32], implying that SPF mice would have limited adaptive immune response to this pathogen, we pretreated wild-type and ILC3$^{\Delta Aire}$ mice for 3 weeks with intravenous (*i.v.*) injections of HKCA, before *i.v.* administration of live *C. albicans*. ILC3$^{\Delta Aire}$ mice were significantly more susceptible to *C. albicans* challenge, with only ~10% survival at 14 days post-challenge, compared to wild-type littermates, which had a ~50% survival rate at this time point (Fig. 5a). Moreover, the ILC3$^{\Delta Aire}$ mice showed a significantly higher burden of *C. albicans* in their kidneys in comparison to wild-type littermate controls (Fig. 5b, c and Extended Data Fig. 3g, h). Similarly, *Aire*$^{-/-}$ mice on either B6 or NOD genetic backgrounds had significantly lower survival rate following *i.v.* injection of live *C. albicans* (with 20% and 0% survival respectively) compared to their *Aire*$^{+/+}$ littermates (with 60% and 45% survival respectively) (Extended Data Fig. 3e-f). While the Aire$^{-/-}$ mice on the B6 background had significantly poorer survival rate than their wild-type littermates, they did not develop detectable levels of IL-17- and/or IL-22-specific autoantibodies (Extended Data Fig. 3i-j), further suggesting that the impaired anti-candida response was primarily T cell dependent.

Next, we assessed the adaptive immune response to live *C. albicans* in a mucosal model of infection. We used a modified version of an existing protocol[33], which is based on the oral administration of live *C. albicans* to mice in 3 consecutive times with 1 day intervals, resulting in a long-lasting colonization of their gastro-intestinal tract. First, we assessed whether oral candida colonization of wild-type mice resulted in the expansion of candida-specific T cells in the secondary lymphoid organs (SLO) (Fig. 6a, b; Extended Data Fig. 4 a, b). Flow cytometry indicated that while wild-type mice not treated with oral *C. albicans* harbored relatively low numbers of Als1-Tet^{+} T cells (3-5 naïve CD44^{-} T cells/SLO in each mouse analyzed), the number of Als1-Tet^{+} T

cells increased by ~50-100-fold at day 14 post *C. albicans* colonization (Fig. 6a, b), and virtually all of them had an activated memory phenotype, as evidenced by high expression of CD44 (Fig. 6a). In contrast, *C. albicans* colonization of ILC3$^{\Delta Aire}$ mice (Fig. 6c, d), Aire$^{-/-}$ mice (Extended Data Fig. 4c-e) or bone-marrow chimeric mice in which Aire deficiency occurred in the hematopoietic, but not in the stromal compartment (Extended Data Fig. 4f-h), resulted in significantly decreased numbers of Als1-Tet^{+} T cells in the SLO than did *C. albicans* colonization of their corresponding wild-type littermate controls. Moreover, low numbers of Als1-Tet^{+} T cells were also observed in CD90.2 Rag1$^{-/-}$ mice that were adoptively transferred with CD90.1^{+} T cells and B cells and treated with a CD90.2-specific antibody to deplete the endogenous CD90.2 lymphoid compartment, thus rendering them ILC-deficient [34] compared to isotype control-treated mice (Extended Data Fig. 4j-k).

We next investigated the presence of candida-specific T cells at different mucosal sites of the gastrointestinal tract at day 1 or day 14 post *C. albicans* administration. While Als1-Tet^{+} T cells could not be detected in the oral cavity, esophagus or small intestine mucosa from wild-type, Aire$^{-/-}$ or ILC3$^{\Delta Aire}$ mice 24 hours post *C. albicans*-challenge (Extended Data Fig. 5), they were present in these locations in wild-type mice at day 14 post-challenge (Fig. 6g, h; Extended Data Fig. 5). In contrast, ILC3$^{\Delta Aire}$ or *Aire*$^{-/-}$ mice had markedly reduced numbers of Als1-Tet^{+} T cells at these sites along the gastrointestinal tract, in particular in the lamina propria, at day 14 post-challenge compared to their corresponding wild-type controls (Fig. 6g, h; Extended Data Fig. 5). In addition, the number of the bulk Rorγt^{+} T_H17 population in pLN and mLN isolated was higher in wild-type mice compared to ILC3$^{\Delta Aire}$ mice at day 14 post *C. albicans* colonization (Extended Data Fig. 6). In contrast the number of Rorγt^{+} T_H17 cells within lamina propria were similar in wild-type mice and ILC3$^{\Delta Aire}$ mice at this time point (Fig. 6i,k), suggesting that while ILC3-specific Aire deficiency impaired the expansion of candida-specific T_H17 cells in the lymphoid organs and lamina propria, the effect on the general T_H17 population was smaller and more variable. In line with the decreased

number of candida-specific T cells at mucosal surfaces, the *Aire*$^{-/-}$ and ILC3$^{\Delta Aire}$ mice had a significantly higher burden of *C. albicans* in their gastrointestinal mucosal sites compared to their wild-type littermates at day 14 post-challenge (Fig. 6k, l; Extended Data Fig. 7).

Finally, we also utilized a more conventional model for oropharyngeal candidiasis (OPC)[35], in which the oral mucosal tissue in mice was exposed to live *C. albicans* for 90 minutes. In this setting, we pre-treated wild-type and ILC3$^{\Delta Aire}$ mice with *i.v.* injection of HKCA every 2 days for 14 days prior to the OPC challenge with live *C. albicans*, and the oral mucosa was analyzed at day 5 after the OPC challenge (Extended Data Fig. 8a). At this timepoint, we observed significantly less Als1-Tet^{+} T cells (Extended data Fig. 8b,c) and a higher burden *C. albicans* (Fig. 6m) in the oral mucosa of ILC3$^{\Delta Aire}$ compared to wild-type mice (Extended Data Fig. 7b,c). Collectively, these data demonstrated that Aire expression in Aire^{+} ILC3s was required for the induction of adaptive immune responses to *C. albicans* at the mucosal surfaces.

Aire^{+} ILC3 induce survival of candida-specific T$_{H}$17 clones

To explore how expression of Aire in Aire^{+} ILC3s promoted the expansion of *C. albicans* specific T cells, we assessed the impact of Aire deficiency on the gene expression profiles of Aire^{+}ILC3s and candida-specific T cells in response to *C. albicans* challenge. For this purpose, we crossed *Aire*$^{-/-}$ mice with *Aire*-GFP reporter mice, to generate *Aire*-GFP-*Aire*$^{-/-}$ mice. Aire^{+} ILC3s sorted (based on *Aire*-GFP expression) from *Aire*-GFP-*Aire*$^{-/-}$ or *Aire*-GFP-*Aire*$^{+/+}$ littermates that had received HKCA or PBS *i.v.* every day for 3 days (Extended Data Fig. 9) were analyzed by bulk RNAseq analysis on day 4. Analysis of these transcriptomes indicated that Aire regulated the expression of hundreds of genes, which strongly overlapped with the genes upregulated in response to *HKCA* (Fig. 7a, b). Specifically, the Aire^{+} ILC3s isolated from HKCA-stimulated *Aire*-GFP-*Aire*$^{-/-}$ mice had impaired induction of genes encoding cytokines (*Il6, Il18, Bmp2), C. albicans*-sensing

receptors (*Clec7a*,), cell adhesion molecules (*Vcam1, Cadm1*), co-stimulatory molecules (*Cd86*) and enzymes involved in proinflammatory response (*Ptgs2*) compared to their HKCA-stimulated *Aire*-GFP-*Aire*$^{+/+}$ counterparts (Fig 7a, b). These data suggested that Aire regulated the expression of several key molecules that may be critical for T_H17 differentiation (*Il6*), T cell clonal expansion (*Cd80/Cd86; Vcam1*) and pro-inflammatory signaling (*Il18, Ptgs2*).

To investigate how Aire deficiency impacted the transcriptional program of *C. albicans*-specific T cells, we adoptively transferred *Rorc*-GFP$^+$ OT-II T cells into wild-type or ILC3$^{\Delta Aire}$ mice that were stimulated with HKCA-OVA or HKCA every second day. *Rorc*-GFP$^+$ OT-II T cells were then isolated from pLN on day 7 post-transfer and analyzed by bulk RNA sequencing (Extended Data Fig. 10a). At this time point, the frequencies of *Rorc*-GFP$^+$ OT-II T cells in ILC3$^{\Delta Aire}$ mice were decreased by ~3-fold compared to wild-type littermates (Extended Data Fig. 10b). We observed only mild increase in the frequency of CPD$^+$ proliferating *Rorc*-GFP$^-$ OT-II T cells in wild-type vs ILC3$^{\Delta Aire}$ mice (Extended Data Fig. 10b), suggesting that Aire was not involved in the regulation of *Rorc*-GFP$^-$ T cell priming.

The transcriptional analysis indicated that the *Rorc*-GFP$^+$ OT-II T cells had substantially different transcriptomes compared to the non-proliferating CPD$^-$ OT-II T cells. Specifically, the *Rorc*-GFP$^+$ OT-II T cells isolated from wild-type mice upregulated 551 genes, including *Rorc, Cd44,* chemokine receptor *Ccr5* and proliferation marker *Mki67* and downregulated 220 genes, including *Sell* and *Cd69*, compared to the non-proliferating CPD$^-$ OT-II T cells from wild-type mice (Fig. 7C and Extended Data Fig. 10b), highlighting their activated/memory phenotype and readiness to exit the lymph node and move to the effector site. We detected more than a thousand differentially expressed genes between the *Rorc*-GFP$^+$ OT-II T cells derived from the wild-type compared to the ILC3$^{\Delta Aire}$ mice (Fig 7c, and Extended Data Fig. 10b). Specifically, *Rorc*-GFP$^+$ OT-II T cells isolated from ILC3$^{\Delta Aire}$ mice had significantly reduced expression of anti-apoptotic factors such as survivin (*Birc5*) or *Bcl2l12*[36] and a less activated/memory phenotype, as suggested by the decreased

expression of the chemokine receptor *Cxcr3*, *Il2rb* (encoding the IL-2 receptor beta subunit), *Igf2r* [37], *Il12rb1* (the key subunit of IL-23 receptor; Fig 7d, e*)* and *Cd28*, encoding the CD80/86 receptor essential for T cell co-stimulation (Fig. 7e). The GO annotation of cell processes indicated that the differentially regulated genes we highly enriched for factors involved in the regulation of cell cycle and/or mitosis (Fig. 7f). Collectively, these data suggested that Aire controlled the expression of genes in Aire$^+$ ILC3s (e.g. *Il6, Cd86, Ptgs2)* that were critical for the subsequent induction of a pro-survival transcriptional program in T_H17 cells (Extended Data Fig. 10d, e).

DISCUSSION

Here we show that extrathymic expression of Aire in Aire$^+$ ILC3s was required for the expansion of candida-specific CD4$^+$ T cells, in particular T_H17 clones, in response to *C. albicans* infection and for consequently limiting the pathogenicity of this opportunistic pathogen at mucosal tissues. We found that Aire$^+$ ILC3s expressed receptors implicated in *C. albicans* detection (e.g. dectin-1, galectin-3) at levels comparable to DCs and effectively endocytosed *C. albicans*. Moreover, upon *C. albicans* uptake, Aire$^+$ ILC3s presented candida-derived antigens to CD4$^+$ T cells through MHCII. Therefore, our study suggests that effective response to *C. albicans* infection involves division of labor between different types of phagocytes and APCs, with Aire$^+$ ILC3s playing a non-redundant role in promoting the survival and subsequent expansion of candida-specific T cell clones in the LN.

While ILCs are generally viewed as the innate analogs of T cells, a growing body of evidence suggests that some ILC subsets are, similarly to Aire$^+$ ILC3, equipped with potent endocytic and/or antigen presentation capacity[38, 39, 40, 41, 42, 43]. For instance, spleen-derived NCR$^-$CCR6$^+$MHCII$^+$ ILC3s, were reported to internalize latex beads and present model protein antigen to CD4$^+$ T cells *in vitro*[43]. Similarly, MHCII$^+$ ILC2 can endocytose and present OVA protein and induce antigen-

specific T cell proliferation[42], while intestinal MHCII$^+$ ILC3s were reported to regulate T cell responses to bacterial antigens in an antigen dependent manner[38, 40, 41], arguing that some ILC3 subsets may act as potent APCs, with the capacity to modulate antigen-specific T cell responses in different contexts and in different anatomical niches[38]. Moreover, our data also suggested that LN-resident MHCII$^-$ ILC3s could upregulate the expression of MHCII and CD86 coding genes in response to *C. albicans* challenge. This is in line with reports showing that the pro-inflammatory cytokine IL-1β promotes the expression of MHCII and costimulatory molecules on spleen-, but not gut-derived MHCII$^-$ ILC3s[43].

Moreover, our data indicated that the impaired expansion of candida-specific CD4$^+$ T cells in SLO of ILC3$^{\Delta Aire}$ mice was associated with their decreased accumulation at different mucosal sites, including the oral cavity, esophagus and intestine, and with increased burden of *C. albicans* at these mucosal tissues. It is likely that the impaired surveillance of the mucosal tissues due to a loss of candida-specific CD4 T cells resulted in reduced ability to control the fungal burden at the mucosal surfaces and loss of barrier integrity. In Aire-deficient patients, in which both the extrathymic and the thymic expression of Aire are defective, additional mechanisms (e.g. autoantibodies against IL-17, IL-22[17, 18, 44], defensins[45] and mucins[46] or loss of Paneth cells [45]) may further impair the integrity of mucocutaneous surfaces and thereby enhance the invasiveness of *C. albicans*. Therefore, the increased susceptibility to *C. albicans* in Aire-deficiency may combine aspects of the role of Aire in central tolerance with its role in shaping the *C. albicans*-specific T_H17 response in the periphery.

Although our data are in line with the interpretation that the increased susceptibility to candida infection in both humans and mice is due to defects in the T_H17 response [12, 14, 15, 47, 48], it was also suggested that in the oral mucosa, Aire-deficient mice and humans have intact T_H17 responses to *C. albicans* and that these phenotypes are due to overproduction of interferon-γ (IFN-γ) in CD4$^+$ and CD8$^+$ T cells at the epithelial barriers[49]. In this specific study, however, the T_H17 response was measured only 24 hours post *C. albicans* challenge [49], which might be too early a

timepoint to assess an adaptive immune response, because *C. albicans* is virtually absent in mice housed under SPF conditions[32, 33]. Indeed, we found that the induction of candida-specific T cells in SPF-housed mice peaked only two weeks post *C. albicans* colonization. In addition, the report assessed bulk T_H17 cell responses[49], and not candida-specific T cell clones as it was done in this study.

The molecular features of Aire$^+$ ILC3s described here seem to largely overlap with a subset of Lin^{neg}*Aire*$^+$*Rorc*$^+$MHCII$^+$ Janus cells that was recently identified using single-cell RNA profiling of mouse LN[50], suggesting they might represent the same cell population. Although the study suggested that the Lin^{neg}*Aire*$^+$*Rorc*$^+$MHCII$^+$ Janus cells are a subset of tolerogenic DCs[50], they lacked expression of key DC canonical markers such as *Cd11c, Cd11b, Dec205, Clec9a* or *Cd4/Cd8*[50], as well as of other key myeloid or lymphoid markers. Moreover, similarly to Aire$^+$ ILC3s, the Janus cells highly expressed ILC3 markers, including *Rorc, Il1r1, c-Kit, il7r, Id2, Ccr6, Ccr7, Il18r1,* as well as genes linked to antigen presentation and co-stimulation. Therefore, although both Aire$^+$ ILC3 and Janus cells lacked the expression of key ILC3 effector molecules such as *Il17a, Il17f* or *Il22,* they bore molecular features more characteristic of MHCII$^+$ innate lymphoid cells, rather than of myeloid APCs. This notion is also supported by a recent study showing that extrathymic Lin^{neg}*Aire*$^+$*Rorc*$^+$ MHCII$^+$ cells have an interconverting potential with ILC3s in a fate mapping analysis based on *Aire*-Cre reporter mice[51]. Irrespectively of nomenclature, our study provides experimental evidence that the expression of Aire in LN-resident Lin^{neg}*Aire*$^+$*Rorc*$^+$ MHCII$^+$ cells has a critical and a non-redundant role in the induction of candida-specific T cells and the control of *C. albicans* colonization at mucosal tissues.

Collectively, our data not only help shedding more light on the mechanisms underlying chronic mucocutaneous candidiasis in Aire-deficient individuals, but also help identifying an additional

functional role for Aire, beyond its well-established role in central tolerance induction in the thymus.

ACKNOWLEDGMENTS

Research in the Abramson laboratory is kindly supported by the European Research Council ERC-2016-CoG-724821; Israel Science Foundation (1796/16 and 1819/21); Chan Zuckerberg Initiative; Bill and Marika Glied and Family Fund, Binational Science Foundation (BSF); Pasteur-Weizmann Delegation; Enoch Foundation, Ruth and Samuel David Gameroff Family Foundation; Erica Drake Fund and Lilly Fulop Fund for Multiple Sclerosis Research. JD was supported by the Dean of Faculty Fellowship by Weizmann Institute of Science and by the Weizmann Institute of Science – Czech Academy of Sciences Bilateral Fellowship by Czech Academy of Sciences, JD, KK, HB and EV are also supported by Charles University PRIMUS grant (Primus/21/MED/003) and Czech Science Foundation JUNIOR STAR grant (21-22435M). BEO and ESH are supported by the K.G. Jebsen Center for autoimmune disorders, The Norwegian Research Council, The Novonordisk Foundation and the Regional Health Authorities of Western Norway. DF is supported by Grant Agency of the Czech Republic (GACR; 17-25365S).

AUTHORS CONTRIBUTION

JA and JD conceived the project, designed the experiments and wrote the manuscript; JD performed the experiments and analyzed the data; JA supervised the study; AB, YG, OB-N, NK, YG, TG, IZ, HB, KK, EV, BEO and ESH assisted at different aspects of the study, including data or sample acquisition and analysis. DF contributed by the essential reagent. LSB and ZS performed the two-photon microscopy and analyzed the data.

CFI statement : The authors declare that they have no conflict of interest

FIGURE LEGENDS

Figure 1| Aire$^+$ ILC3s express *C. albicans* sensing receptors.

a) FACS sorting strategy of cILC3s, MHCII$^+$ ILC3s and Aire$^+$ ILC3s subsets isolated from the popliteal lymph nodes of *Rorc*^{tdTomato} *Aire*^{GFP} reporter mice. Representative plots are shown. **b)** Heatmap of Pearson correlation according to gene expression values between individual samples as in a). **c-f**) RNA-seq based heatmap of expression of lineage specific genes (**c**), genes associated with MHCII-presentation or co-stimulation (**d**), genes encoding receptors implicated in sensing and/or phagocytosis of *C. albicans* (**e**) and genes encoding signaling molecules downstream of *C. albicans* sensing receptors (**f**) in cILC3s, MHCII$^+$ ILC3s, Aire$^+$ ILC3s and MHCII$^+$ CD11c$^+$ DCs isolated from popliteal lymph nodes of *Rorc*^{tdTomato} *Aire*^{GFP} at steady-state. **g)** Flow cytometry of Rorγt$^+$ cILC3s, Rorγt$^+$ MHCII$^+$ ILC3s, Rorγt$^+$ MHCII$^+$Aire$^+$ ILC3s and MHCII$^+$ CD11c$^+$ DCs isolated from popliteal lymph nodes of wild-type animals under steady-state conditions. Grey filled histogram indicates staining in control dectin-1 or galectin-3-deficient mice or isotype control for CD80, CD86, TLR2. Representative figure, n≥3.

Figure 2| *C. albicans* induces transcriptional changes in ILC3 subsets

a-c) Volcano plots of bulk RNA-seq analyses showing differential gene expression in non-stimulated vs. HKCA stimulated cILC3 **(a)**, MHCII$^+$ ILC3 **(b)** and Aire$^+$ ILC3 **(c)** subpopulations isolated from the popliteal lymph nodes of *Rorc*^{tdTomato} *Aire*^{GFP} mice *i.v.* injected by HKCA or PBS for three consecutive days, using gating strategy as in Fig. 1a. Dashed lines indicate the cutoff for fold-change (Fc)=2.0 and p-value=0.05. Wald test was used to calculate the p-value. Based on their function, the selected genes were highlighted in blue (antigen presentation, co-stimulation), red (cytokine and chemokine signaling), green (candida sensing receptors), purple (*Aire*); **d)** Fold change:fold change (Fc:Fc) graph of RNA-seq data showing differential gene expression in Aire$^+$ ILC3s in contrast to stimulated or non-stimulated MHCII$^+$ ILC3s. Comparison of fold-change of Aire$^+$ ILC3s vs. MHCII$^+$ ILC3s (x-axis) and non-stimulated vs. HKCA stimulated MHCII$^+$ ILC3s (y-axis) isolated by FACS using a gating strategy as in Fig. 1a. Dashed lines indicate the Fc=2.0 cutoff. **e)** RNA-seq-based heatmap showing the level of expression of selected effector genes in ILC3s, MHCII$^+$ ILC3s and Aire$^+$ ILC3s with or without HKCA stimulation. Data are plotted as the z-score calculated for particular row. Data are derived from three independent biological replicates for each population (a-e).

Figure 3| Aire$^+$ ILC3s internalize *C. albicans* for antigen presentation

a-b) Imaging flow cytometry showing the physical interaction between HKCA and Aire$^+$ ILC3s isolated from popliteal lymph nodes of wild-type mice and incubated ex-vivo with CPD-stained HKCA for 30 (**a**) or 90 minutes (**b**). Samples were stained for Aire and DAPI (**a-b**) and MHCII (**b**). Shown are representative images of one out of five independent experiments. Scale bar: 8µm. **c-f)** *In vitro* reporter assay measuring the capacity of B cells, Ly6C$^+$ MNPs, CD11b$^+$ MNPs, CD11c$^+$ MNPs and Aire$^+$ ILC3s to endocytose HKCA transgenically expressing OVA (HKCA-OVA) either *in vitro* **(c)** or *in vivo* **(d-f)** and subsequently to present HKCA-derived OVA antigens on their MHCII molecules to DO11.10-TCR NFAT-GFP reporter cell line that was co-incubated with the sorted populations for 17 hours. The corresponding APC populations were FACS-sorted according to gating strategy shown in Extended Data Fig. 3a, b. Antigen presentation capacity was measured as a frequency of NFAT-GFP$^+$ reporters in the specific sample. Representative data set out of three independent experiments are shown (n=5 for each experiment), mean ± SD depicted. (**d-f)** Dot plot of B cells, Ly6C$^+$ MNPs, CD11b$^+$ MNPs, CD11c$^+$ MNPs and Aire$^+$ ILC3s depicting APC capacity at 12 hours (**d**), 24 hours (**e**) or 72 hours (**f**) after HKCA-OVA i.v. injection of HKCA-OVA into wild-type mice; **g)** Two-photon microcopy of explanted popliteal lymph nodes showing interaction between *Aire*-GFP$^+$ cells and candida-specific T cells from *Aire*-GFP reporter mice adoptively transferred with OT-II^{tdTomato} T cells stimulated by either HKCA or HKCA-OVA. Representative figures from two experiments are shown.

Figure 4| Aire$^+$ ILC3s are essential for the generation of *C. albicans*-specific T$_H$17 response

a) Flow cytometry analysis showing disruption of *Aire*-expression *Rorc*-Cre$^-$Aire$^{fl/fl}$ (WT) and *Rorc*-Cre$^+$Aire$^{fl/fl}$ **(**ILC3$^{\Delta Aire}$) mice. Shown are representative FACS plots (n≥6) of intracellular Aire-staining of thymic stroma (upper panel) or lineage negative cells from pLNs (lower panel); **b-e)** Flow cytometric analysis of OT-II T cell proliferation and differentiation in WT or ILC3$^{\Delta Aire}$ mice transferred with naïve OT-II and control CD4$^+$ T cells in 1:1 ratio and subsequently injected with HKCA or HKCA-OVA every second day for 2 weeks showing representative flow cytometry dot plot show the frequencies of transferred CD45.1$^+$ OT-II T cell vs. CD45.1/CD45.2 double positive control T cell populations on day 14 post-transfer **(b),** the corresponding statistical analysis showing ratios (mean ± SD, two-tailed Student´s t-test) of OT-II vs. control T cells (n=5 per group) **(c)**, the frequencies of OT-II *Rorc*-GFP$^+$ cells **(d)** and the corresponding statistical analysis of the

experiment showing the total counts (mean ± SD, two-tailed Student´s t-test) of HKCA-induced OT-II *Rorc*-GFP^{+} cells **(e)**; **f-g**, Flow cytometric analysis assessing counts of Als1-tetramer positive CD4 T cells in WT, ILC3$^{\Delta Aire}$ and TEC$^{\Delta Aire}$ mice that were injected intravenously with HKCA every second day for two weeks showing representative FACS plot **(f)** and the corresponding statistical analysis depicting the total counts (mean ± SD, two-tailed Student´s t-test) in all mice (n=5) **(g)**; **h-i)** Flow cytometric analysis assessing the proliferation of human RorγT^{+} T$_{H}$17 cells in PBMCs isolated from APS-1 patients or healthy controls showing representative dot plots of the frequency of proliferating RorγT^{+} T$_{H}$17 cells measured by CPD dilution (**h)** and the corresponding statistical analysis of the experiment depicting average frequency (mean ± SD, two-tailed Student´s t-test, n=10 per group) **(i); j)** ELISA assessing amounts of IL-17A in the PBMC supernatants from proliferation assay described in **(h)**. Data are shown as mean of IL-17A concentration ± SD, n=10 for each group, two-tailed Student´s t-test. P-value indicators: *** = p-value < 0.0001, ** = p-value < 0.001, * = p-value < 0.05, ns = not significant.

Figure 5| Mice lacking extrathymic expression of Aire have reduced survival after systemic challenge with live *C. albicans*

a) Survival curves of WT (Cre^{-}Aire$^{fl/fl}$) and ILC3$^{\Delta Aire}$ (*Rorc*-Cre^{+}Aire$^{fl/fl}$) mice (n≥10 per genotype group) injected *i.v.* with HKCA every two days for three weeks prior the infection by live *C. albicans*. Long-rank (Mantel-Cox) test was used to calculate the p-value: 0.0414; **b)** Quantitative PCR analysis of *C. albicans*-specific DNA in the kidney from WT and ILC3$^{\Delta Aire}$ mice (n=6) infected with *C. albicans* as in a (mean ± SD, two-tailed Student´s t-test); **c)** Colony forming units (CFU)-based assay determining the overgrowth of *C albicans* in kidneys of mice described in (a), (n=6, mean ± SD, two-tailed Student´s t-test). P-value indicators: *** = p-value < 0.0001, ** = p-value < 0.001, * = p-value < 0.05, ns = not significant.

Figure 6| Extrathymic expression of Aire is critical for an effective T$_{H}$17 response to *C. albicans* at mucosal sites

a-b) Flow cytometry analysis assessing frequencies of *C. albicans*-specific Als1-Tet^{+}, CD4^{+} T cells in pLNs of WT mice orally colonized by *C. albicans* and analyzed at different time points post colonization. Representative FACS plot showing counts of Als1-tet^{+}, *C. albicans*-specific CD4^{+} T cells (highlighted in red rectangles in the upper panel and red dots in the lower panel showing T cell activation markers CD44 vs CD69) **(a)** with a corresponding statistical analysis of the same

experiment showing the total counts (mean +SD, two-tailed Student´s t-test **(b)**; **c-j**) Flow cytometry analysis assessing frequencies of *C. albicans*-specific Als1-Tet^{+}, CD4^{+} T cells in pLNs **(c-f)** or intestinal lamina propria **(g-j)** of WT vs. ILC3$^{\Delta Aire}$ mice orally colonized by *C. albicans* and analyzed two weeks post colonization. Representative FACS dot plots showing counts of tetramer positive CD4 T cells (**c, g**) and RorγT^{+} CD4 T cells (**e, i**) are highlighted in black and red rectangles respectively. Statistical analyses showing the total counts (mean +SD, two-tailed Student´s t-test, n=6 per group) corresponding to data shown in (**c, e, g, i**) are shown in (**d, f, h, j**) respectively. Representative experiment out of three independent biological replicates is shown. (**k)** Quantitative PCR analysis assessing the presence of *C. albicans*-specific DNA in the ileal part of small intestine from WT and ILC3$^{\Delta Aire}$ mice (mean +SD, two-tailed Student´s t-test, n=6 per group). **l)** Colony forming units (CFU)-based assay determining the overgrowth of *C albicans* in small intestinal tissues 14 days after oral colonization (mean +SD, two-tailed Student´s t-test, n=6 per group). **m)** CFU-based assay determining the overgrowth of *C albicans* in oral mucosa 6 days after OPC challenge (mean +SD, two-tailed Student´s t-test, n=6 per group). P-value indicators: *** = p-value < 0.0001, ** = p-value < 0.001, * = p-value < 0.05, ns = not significant.

Figure 7| Aire^{+} ILC3s induce pro-survival program in candida-specific T$_{H}$17 clones

a) Volcano plot of bulk RNA-seq analysis showing differential gene expression in Aire^{+} ILC3s that were isolated from pLN of HKCA-stimulated *Aire*^{GFP}*Aire*$^{+/+}$ vs *Aire*^{GFP}*Aire*$^{-/-}$ mice. Dashed lines indicate the Fc=2.0 and p-value=0.05 cutoff. Selected genes are highlighted in blue (antigen cell adhesion, co-stimulation), red (cytokine and chemokine signaling), green (candida sensing receptors). **b)** Fold change:fold change (Fc:Fc) graph of RNA-seq data showing differential gene expression in Aire^{+} ILC3s promoted by HKCA stimulation. Comparison of fold-change of HKCA-stimulated vs. non-stimulated Aire^{+} ILC3s isolated from *Aire*^{GFP}*Aire*$^{+/+}$ vs *Aire*^{GFP}*Aire*$^{-/-}$ (x-axis) and Aire^{+} ILC3s from stimulated *Aire*^{GFP}*Aire*$^{+/+}$ vs stimulated *Aire*^{GFP}*Aire*$^{-/-}$ (y-axis). **c)** Volcano plot of RNA-seq data showing differential gene expression of *Rorc*-GFP^{+} versus non-proliferating OT-II T cells derived from WT **(***Rorc*-Cre^{-}*Aire*$^{fl/fl}$) versus ILC3$^{\Delta Aire}$ (*Rorc*-Cre^{+}*Aire*$^{fl/fl}$) mice. The mice were transferred with naïve OT-II CD4^{+} T cells and subsequently injected with HKCA-OVA four times during a single week; **d)** Volcano plot of RNA-seq data showing differential gene expression of *Rorc*-GFP^{+} OT-II T cells derived from WT versus ILC3$^{\Delta Aire}$ mice treated as in (**c**). Dashed lines indicate the Fc=2.0 and p-value=0.05 cutoff. Data are derived from three independent replicates. (**e)** RNA-Seq based heatmap showing the level of expression of selected genes in *Rorc*-GFP^{+} OT-II T cells isolated from WT and ILC3$^{\Delta Aire}$ mice. Data are plotted as the z-score calculated

for particular row. (**f**) GO enrichment for upregulated differentially expressed genes from *Rorc*-GFP^{+} OT-II T cells derived from WT versus ILC3$^{\Delta Aire}$ mice.

REFERENCES

1. Anderson, M.S. *et al.* Projection of an immunological self shadow within the thymus by the aire protein. *Science* **298**, 1395-1401 (2002).

2. Klein, L., Kyewski, B., Allen, P.M. & Hogquist, K.A. Positive and negative selection of the T cell repertoire: what thymocytes see (and don't see). *Nat Rev Immunol* **14**, 377-391 (2014).

3. Liston, A., Lesage, S., Wilson, J., Peltonen, L. & Goodnow, C.C. Aire regulates negative selection of organ-specific T cells. *Nat Immunol* **4**, 350-354 (2003).

4. Aschenbrenner, K. *et al.* Selection of Foxp3+ regulatory T cells specific for self antigen expressed and presented by Aire+ medullary thymic epithelial cells. *Nat Immunol* **8**, 351-358 (2007).

5. Malchow, S. *et al.* Aire Enforces Immune Tolerance by Directing Autoreactive T Cells into the Regulatory T Cell Lineage. *Immunity* **44**, 1102-1113 (2016).

6. Abramson, J. & Husebye, E.S. Autoimmune regulator and self-tolerance - molecular and clinical aspects. *Immunol Rev* **271**, 127-140 (2016).

7. Husebye, E.S., Anderson, M.S. & Kämpe, O. Autoimmune Polyendocrine Syndromes. *N Engl J Med* **378**, 2543-2544 (2018).

8. Bruserud, Ø. *et al.* A Longitudinal Follow-up of Autoimmune Polyendocrine Syndrome Type 1. *J Clin Endocrinol Metab* **101**, 2975-2983 (2016).

9. Perheentupa, J. Autoimmune polyendocrinopathy-candidiasis-ectodermal dystrophy. *J Clin Endocrinol Metab* **91**, 2843-2850 (2006).

10. Okada, S. *et al.* IMMUNODEFICIENCIES. Impairment of immunity to Candida and Mycobacterium in humans with bi-allelic RORC mutations. *Science* **349**, 606-613 (2015).

11. Puel, A. *et al.* Chronic mucocutaneous candidiasis in humans with inborn errors of interleukin-17 immunity. *Science* **332**, 65-68 (2011).

12. Milner, J.D. *et al.* Impaired T(H)17 cell differentiation in subjects with autosomal dominant hyper-IgE syndrome. *Nature* **452**, 773-776 (2008).

13. Ferwerda, B. *et al.* Human dectin-1 deficiency and mucocutaneous fungal infections. *N Engl J Med* **361**, 1760-1767 (2009).

14. Glocker, E.O. *et al.* A homozygous CARD9 mutation in a family with susceptibility to fungal infections. *N Engl J Med* **361**, 1727-1735 (2009).

15. Liu, L. *et al.* Gain-of-function human STAT1 mutations impair IL-17 immunity and underlie chronic mucocutaneous candidiasis. *J Exp Med* **208**, 1635-1648 (2011).

16. Conti, H.R. & Gaffen, S.L. IL-17-Mediated Immunity to the Opportunistic Fungal Pathogen Candida albicans. *J Immunol* **195**, 780-788 (2015).

17. Kisand, K. *et al.* Chronic mucocutaneous candidiasis in APECED or thymoma patients correlates with autoimmunity to Th17-associated cytokines. *J Exp Med* **207**, 299-308 (2010).

18. Puel, A. *et al.* Autoantibodies against IL-17A, IL-17F, and IL-22 in patients with chronic mucocutaneous candidiasis and autoimmune polyendocrine syndrome type I. *J Exp Med* **207**, 291-297 (2010).

19. Yamano, T. *et al.* Aire-expressing ILC3-like cells in the lymph node display potent APC features. *J Exp Med* **216**, 1027-1037 (2019).

20. Schlitzer, A. *et al.* IRF4 transcription factor-dependent CD11b+ dendritic cells in human and mouse control mucosal IL-17 cytokine responses. *Immunity* **38**, 970-983 (2013).

21. Jouault, T. *et al.* Candida albicans phospholipomannan is sensed through toll-like receptors. *J Infect Dis* **188**, 165-172 (2003).

22. Blasi, E. *et al.* Biological importance of the two Toll-like receptors, TLR2 and TLR4, in macrophage response to infection with Candida albicans. *FEMS Immunol Med Microbiol* **44**, 69-79 (2005).

23. Brown, G.D. *et al.* Dectin-1 mediates the biological effects of beta-glucans. *J Exp Med* **197**, 1119-1124 (2003).

24. Gantner, B.N., Simmons, R.M. & Underhill, D.M. Dectin-1 mediates macrophage recognition of Candida albicans yeast but not filaments. *EMBO J* **24**, 1277-1286 (2005).

25. Kohatsu, L., Hsu, D.K., Jegalian, A.G., Liu, F.T. & Baum, L.G. Galectin-3 induces death of Candida species expressing specific beta-1,2-linked mannans. *J Immunol* **177**, 4718-4726 (2006).

26. Jouault, T. *et al.* Specific recognition of Candida albicans by macrophages requires galectin-3 to discriminate Saccharomyces cerevisiae and needs association with TLR2 for signaling. *J Immunol* **177**, 4679-4687 (2006).

27. Veldhoen, M., Hocking, R.J., Atkins, C.J., Locksley, R.M. & Stockinger, B. TGFbeta in the context of an inflammatory cytokine milieu supports de novo differentiation of IL-17-producing T cells. *Immunity* **24**, 179-189 (2006).

28. Bettelli, E. *et al.* Reciprocal developmental pathways for the generation of pathogenic effector TH17 and regulatory T cells. *Nature* **441**, 235-238 (2006).

29. Mangan, P.R. *et al.* Transforming growth factor-beta induces development of the T(H)17 lineage. *Nature* **441**, 231-234 (2006).

30. Dobeš, J. *et al.* A novel conditional Aire allele enables cell-specific ablation of the immune tolerance regulator Aire. *Eur J Immunol* **48**, 546-548 (2018).

31. Eberl, G. & Littman, D.R. Thymic origin of intestinal alphabeta T cells revealed by fate mapping of RORgammat+ cells. *Science* **305**, 248-251 (2004).

32. Jiang, T.T. *et al.* Commensal Fungi Recapitulate the Protective Benefits of Intestinal Bacteria. *Cell Host Microbe* **22**, 809-816.e804 (2017).

33. Shao, T.Y. *et al.* Commensal Candida albicans Positively Calibrates Systemic Th17 Immunological Responses. *Cell Host Microbe* **25**, 404-417.e406 (2019).

34. Sonnenberg, G.F., Monticelli, L.A., Elloso, M.M., Fouser, L.A. & Artis, D. CD4(+) lymphoid tissue-inducer cells promote innate immunity in the gut. *Immunity* **34**, 122-134 (2011).

35. Solis, N.V. & Filler, S.G. Mouse model of oropharyngeal candidiasis. *Nat Protoc* **7**, 637-642 (2012).

36. Altieri, D.C. Survivin - The inconvenient IAP. *Semin Cell Dev Biol* **39**, 91-96 (2015).

37. DiToro, D. *et al.* Insulin-Like Growth Factors Are Key Regulators of T Helper 17 Regulatory T Cell Balance in Autoimmunity. *Immunity* **52**, 650-667.e610 (2020).

38. Sonnenberg, G.F. & Hepworth, M.R. Functional interactions between innate lymphoid cells and adaptive immunity. *Nat Rev Immunol* **19**, 599-613 (2019).

39. Hepworth, M.R. *et al.* Innate lymphoid cells regulate CD4+ T-cell responses to intestinal commensal bacteria. *Nature* **498**, 113-117 (2013).

40. Hepworth, M.R. *et al.* Immune tolerance. Group 3 innate lymphoid cells mediate intestinal selection of commensal bacteria-specific $CD4^+$ T cells. *Science* **348**, 1031-1035 (2015).

41. Melo-Gonzalez, F. *et al.* Antigen-presenting ILC3 regulate T cell-dependent IgA responses to colonic mucosal bacteria. *J Exp Med* **216**, 728-742 (2019).

42. Oliphant, C.J. *et al.* MHCII-mediated dialog between group 2 innate lymphoid cells and CD4(+) T cells potentiates type 2 immunity and promotes parasitic helminth expulsion. *Immunity* **41**, 283-295 (2014).

43. von Burg, N. *et al.* Activated group 3 innate lymphoid cells promote T-cell-mediated immune responses. *Proc Natl Acad Sci U S A* **111**, 12835-12840 (2014).

44. Kärner, J. *et al.* Anti-cytokine autoantibodies suggest pathogenetic links with autoimmune regulator deficiency in humans and mice. *Clin Exp Immunol* **171**, 263-272 (2013).

45. Dobeš, J. *et al.* Gastrointestinal Autoimmunity Associated With Loss of Central Tolerance to Enteric α-Defensins. *Gastroenterology* **149**, 139-150 (2015).

46. Gavanescu, I., Kessler, B., Ploegh, H., Benoist, C. & Mathis, D. Loss of Aire-dependent thymic expression of a peripheral tissue antigen renders it a target of autoimmunity. *Proc Natl Acad Sci U S A* **104**, 4583-4587 (2007).

47. Ma, C.S. *et al.* Deficiency of Th17 cells in hyper IgE syndrome due to mutations in STAT3. *J Exp Med* **205**, 1551-1557 (2008).

48. Minegishi, Y. *et al.* Human tyrosine kinase 2 deficiency reveals its requisite roles in multiple cytokine signals involved in innate and acquired immunity. *Immunity* **25**, 745-755 (2006).

49. Break, T.J. *et al.* Aberrant type 1 immunity drives susceptibility to mucosal fungal infections. *Science* **371** (2021).

50. Wang, J. *et al.* Single-cell multiomics defines tolerogenic extrathymic Aire-expressing populations with unique homology to thymic epithelium. *Sci Immunol* **6**, eabl5053 (2021).

51. Lyu, M. *et al.* ILC3s select for RORγt⁺ Tregs and establish tolerance to intestinal microbiota. *bioRxiv*, 2022.2004.2025.489463 (2022).

MATERIAL AND METHODS

Mice

The Aire$^{fl/fl}$ (Jax: 031409;[30]), Aire$^{-/-}$ (004743 C57BL/6J and 006360 NOD genetic background;[1] and[52]), *Aire*-GFP (*Aire*-IGRP-GFP;[53]) a kind gift of Dr. M. S. Anderson (University of California, San Francisco, USA), CD45.1 congenic strain (002014), CD90.1 congenic strain (000406), *Clec7a*$^{-/-}$ (012337,[54]), *Foxn1*-Cre (018448,[55]), *Lgals3*$^{-/-}$ (006338,[56]), OT-II (004194;[57]), Rag1$^{-/-}$ (002216;[58]) *Rorc*-Cre (022791;[31]), *Rorc*-GFP (007572;[31]), *Rosa*-tdTomato (007914;[59]) strains were used in the study. Unless indicated otherwise, all mouse strains were of C57Bl6/J genetic background and were purchased from Jackson laboratories if not indicated otherwise. Mice were housed in the premises of Weizmann Institute of Science in SPF conditions. All experiments were approved by local ethical committee (IACUC) under numbers: 39661117-2, 01420218-2, 04690718-2, 14850619-2. Usually, 6-8 weeks old mice were used for the experiments with the exception of bone marrow chimeras, where mice were 12-15 weeks old. For the generation of bone marrow chimeras, recipients were irradiated by single dose of 900 rad and transplanted by 1.10^7 bone marrow cells. Only mice with reconstitution level higher than 95% were used for experiments. For the generation of CD90-disperate chimeras the protocol described elsewhere was used[34]. Briefly, 6 weeks old Rag1$^{-/-}$ mice were intravenously adoptively transferred by 8.10^7 MACS-enriched T cells and B-cells from CD90.1 mice. These were let to homeostatically proliferate for two months. After this period, mice were intraperitoneally injected by 250µg of CD90.2 depleting antibody (BioXcell) every 3 days. Whenever possible, littermates were used as the controls.

Human samples

Patients were included from Norwegian National Registry of Organ Specific Autoimmune Diseases and fulfilled the APS-1 diagnostic criteria. All APS-1 patients suffer from *C. albicans* infection. Gender matched controls were recruited from the local blood bank at Haukeland University

Hospital. All participants gave informed and written consent, and the study was approved by The Regional Committee for Medical and Health Research Ethics for Western Norway. PBMC were obtained from the whole blood by centrifugation in Ficoll-Pague (GE Healthcare), freeze and stored in liquid nitrogen. The proliferation assay was done for all samples together; whole PBMC fraction (5.10^6 cells) was stained by Cell proliferation dye and stimulated by 1.10^5 HKCA particles (Invivogen). Proliferative response was measured 4 and 6 days later.

Material

All material and reagents used in this study are described in particular relevant section and in detail specified in Suppl. Table 1 and 2.

Infection by live *C. albicans*

Experimental mice were intra-venously injected every two days by 10^6 particles of heat-killed *C. albicans* in PBS for the duration of three weeks. After this period, mice were infected by single dose of 10^5 particles of live *C. albicans*. Mice were then monitored daily for their well-being and were sacrificed when they lose 20% of their initial weight of show signs of distress.

Mucosal colonization by *C. albicans*

In order to establish the gastrointestinal colonization by *C. albicans*, mice were supplemented *ad libitum* by 1mg/ml of ampicillin in drinking water and were kept on it during the experiment. After two days, mice were colonized by 50 ul of 10^6 particles *C. albicans* in PBS. The inoculation was performed dropwise into the mouth of mice. Experimental mice were monitored daily for their well-being.

ELISA

For the detection of autoantibodies, the ELISA microtiter plate was pre-coated by 5µl/ml of recombinant IL-17 or IL-22 in bicarbonate buffer overnight in 4°C. The plate was washed and blocked by 5% milk. Detection of autoantibodies was performed using anti-IgG specific antibody conjugated to HRP (Jackson Immunoresearch). For the detection of human IL-17A cytokine the Human IL-17A ELISA kit (Biolegend) was used according to manufactures instructions.

C. albicans strains and preparation of HKCA

The wild-type *C. albicans* strain used in the study is of SC5314 origin[60]. GFP and OVA coding sequence were inserted in the coding frame after the c-terminal end of the Eno1 gene resulting in generation of OVA-expressing strain derived from the wild-type[61]. Both strains were a kind gift of Dr. Judith Berman (Tel Aviv University, Israel). *C. albicans* was grown in 30°C using YPD agar. HKCA variant was prepared by heat-inactivation of the yeast in 60°C for one hour in thermo-shaker. The heat-inactivation was tested by seeding the HKCA on YPD plates.

Cell isolation for flow cytometry and cell sorting

Aire-ILC3, MHCII-ILC3, ILC3s and DCs were isolated as described previously[19]. Although all systemic LNs were found to contain Aire-ILC3 like cells[19], for consistency most of the experiments was done by analysis of cells and cellular responses in the popliteal LNs, unless stated otherwise. Briefly, lymph nodes were collected and subjected to several rounds of enzymatic digestion by Dispase I. (Roche). Single cell suspension was depleted of lineage positive cells using LS-column based MACS enrichment by cocktail of biotinylated antibodies (TCR-β, CD3, CD19, B220, CD11b, F4/80, Gr1, CD11c, Biolegend) and anti-biotin microbeads (Miltenyi Biotec). T cells were isolated by meshing the skin-draining lymph nodes and spleens through 40 µm nylon mesh. For surface staining, cells were incubated with antibodies for 25 minutes on ice. DAPI (Sigma) of

viability dye eF506 (eBioscience) were used for live/dead cells discrimination. For intracellular staining fixation the Foxp3 / Transcription factor staining buffer set (eBioscience) was used according to manufacturer's recommendation. Subsequently, intracellular targets were stained by antibodies for one hour in room temperature. Cells from the small intestinal lamina propria, oral cavity or esophagus were collected by enzymatic digestion. Briefly, small intestinal tissue was subjected to two rounds of epithelial cells removal by incubation with 2mM EDTA in HBSS for 20 minutes in 37°C. All the tissues were digested in 1mg/ml of Collagenase D and (Roche) for 1 hour and immune cells were enriched by Percoll gradient (Sigma Aldrich). For details concerning antibodies please refer to Suppl. Table 2. Flow cytometry analysis and cell sorting were performed using BD CantoII, LSRII and AriaIII machines (BD). FlowJO (V10; Tristar) software was used for flow cytometry data analysis.

RNA sequencing

Single cell suspensions were directly FACS sorted to Lysis/Binding buffer (Invitrogen) and frozen on dry ice. RNA was isolated using Dynabeads (Invitrogen) according to manufactures protocol. The MARS-seq protocol described elsewhere was followed to generate the sequencing libraries[62]. The sequencing of the library was performed using the NextSeq high output kit and NextSeq 500 sequencer (Ilumina). Obtained data were analyzed for differential gene expression using the UTAP pipeline[63].

Imagestream analysis of endocytosis

Lineage negative cell population or enriched DCs were co-incubated in-test described time period together with Cell proliferation dye eF660 (Thermo) stained 10^5/ml HKCA particles in 37°C. Cells were fixed by Foxp3 / Transcription factor staining buffer set (eBioscience) and stained immediately after the end of incubation period and subjected to Imagestream analysis (Amnis). Data were analyzed using Ideas (v6.2) software (Amnis).

Image acquisition by TPLSM

MACS-isolated tdTomato$^+$ cells were adoptively transferred to *Aire*-GFP hosts and stimulated by heat-killed HKCA or HKCA-OVA. Zeiss LSM 880 upright microscope fitted with Coherent Chameleon Vision laser was used for lymph node imaging experiments. Images were acquired with a femtosecond-pulsed two-photon laser tuned to 930 nm. The microscope was fitted with a filter cube containing 565 LPXR to split the emission to a PMT detector (with a 579-631 nm filter for tdTomato fluorescence) and to an additional 505 LPXR mirror to further split the emission to 2 GaAsp detectors (with a 500-550nm filter for GFP fluorescence). Pictures were acquired at 512 × 512 x-y resolution and the zoom was set to 1.5.

Analysis of endocytosis and antigen presentation capacity by FACS

Experimental mice were intravenously injected by 10^6 Cell proliferation dye eF660 (Thermo) stained HKCA. Mice were analyzed in indicated described time periods. For intravascular staining, mice were injected five minutes prior the analysis intravenously by 5 µg of anti-mouse CD45 BV605 monoclonal antibody (30-F11, Biolegend). For the antigen presentation assays experimental mice were intravenously injected by 10^6 HKCA or HKCA-OVA particles. Cells with antigen presentation capacity were isolated using FACS-sort and incubated with DO11.10 TCR NFAT-GFP cell line[4] for 17 hours in ratio 1:5. GFP-fluorescence was measured using FACS.

Adoptive T cell transfer and stimulation of mice by HKCA

Naïve ovalbumin specific TCR$^+$ OT-II cells from CD45.1$^+$ mice and wild-type derived CD4$^+$ T cells (CD45.1/CD45.2) were isolated using Naïve CD4$^+$ T cells isolation kit (Miltenyi Biotec), mixed in 1:1 ratio, stained by Cell proliferation dye eF660 (Thermo) and transfer via tail vain to recipient mice. Once in two days, mice were injected by 10^6 HKCA or HKCA-OVA particles via tail vein.

Tetramer staining of *C. albicans* specific T cells

Als1 tetramers conjugated with PE and APC were used to detect *C. albicans* specific T cells from HKCA stimulated mice or mice after *C. albicans* colonization. The staining by tetramers and pulldown of tetramer positive cells by anti-PE and anti-APC conjugated microbeads (Miltenyi Biotec) was performed as described elsewhere[64]. Each batch of tetramer reagent was titrated to determine the optimal staining concentration. We thank the NIH Tetramer Core Facility for providing tetramer reagents.

Isolation of DNA from tissue and intestinal content and quantification of *C. albicans* burden

Approximately 3mm of the ileum or kidney or liver tissue were surgically resected including its content. DNA was extracted using Quick-DNA kit (Zymo research) according to manufactures instructions. 10ng of isolated DNA was used for downstream quantitative PCR reaction using Syber -green (Roche) and following set of primers for detection of C. albicans (pF: TTTATCAACTTGTCACACCAGA , pR:ATCCCGCCTTACCACTACCG) and bacterial ribosomal subunit 16S (pF: ACTCCTACGGGAGGCAGCAGT, pR: ATTACCGCGGCTGCTGGC) as the calibrator. The relative C. albicans DNA content in the samples was calculated using method described elsewhere[65].

Isolation of RNA from tissues and quantification of gene expression

Approximately 0.1g of the tongue tissue, esophagus, ileal part of small intestine and kidney was collected and RNA was extracted using Nucleospin RNA Mini kit (Macherey Nagel) according to manufactures instructions. Isolated RNA was subjected to reverse transcription reaction using RevertAid RT Reverse Transcription Kit (Thermo). Quantitative PCR reaction using Syber -green (Roche) and following set of primers was used; *Il17a* (pF: TGACCCCTAAGAAACCCCCA, pR: TCATTGTGGAGGGCAGACAA), *Il17f* (pF: GAAGGCTGGGAACTGTCCTC , pR:

CGGAGTTCATGGTGCTGTCT), *Il22* (pF: TTGACACTTGTGCGATCTCTGA, pR: AAAGGTGCGGTTGACGATGT), and *Casc3* as housekeeping gene (pF: TTCGAGGTGTGCCTAACCA, pR: GCTTAGCTCGACCACTCTGG). The relative gene expression was calculated using method described elsewhere[65].

Mouse model of Oropharyngeal candidiasis (OPC)

Mice were first primed by repeated injection of 10^6 HKCA particles every second day for the duration of two weeks. Then, previously established protocol was followed[35]. Briefly, mice were sedated and exposed to *C. albicans* orally for 1.5 hours using cotton swabs soaked with *C. albicans* diluted in PBS (10^7 particles/ml). Mice were analyzed five days post oral inoculation.

Determination of C. albicans CFU

0.2g of the tongue, esophagus, ileal part of small intestine and kidney tissue was mechanically disrupted in PBS and plated on Sabouraud Dextrose Agar (Merck) in two dilutions. Number of colonies was calculated after 24 and 48 hours. The CFU were recalculated per g of original tissue.

Statistical analysis

Unless indicated otherwise, statistical significance was assessed using two-tailed Student`s *t* test calculated in GraphPad Prism program. For summarizing the p-value, following marks were used: *** = p-value < 0.0001, ** = p-value < 0.001, * = p-value < 0.05, ns = not significant.

Access codes for all transcriptomics data

All RNA-seq data are available at GEO under accession number: GSE203158

Methods references

52. Jiang, W., Anderson, M.S., Bronson, R., Mathis, D. & Benoist, C. Modifier loci condition autoimmunity provoked by Aire deficiency. *J Exp Med* **202**, 805-815 (2005).

53. Gardner, J.M. *et al.* Deletional tolerance mediated by extrathymic Aire-expressing cells. *Science* **321**, 843-847 (2008).

54. Taylor, P.R. *et al.* Dectin-1 is required for beta-glucan recognition and control of fungal infection. *Nat Immunol* **8**, 31-38 (2007).

55. Gordon, J. *et al.* Specific expression of lacZ and cre recombinase in fetal thymic epithelial cells by multiplex gene targeting at the Foxn1 locus. *BMC Dev Biol* **7**, 69 (2007).

56. Colnot, C., Fowlis, D., Ripoche, M.A., Bouchaert, I. & Poirier, F. Embryonic implantation in galectin 1/galectin 3 double mutant mice. *Dev Dyn* **211**, 306-313 (1998).

57. Barnden, M.J., Allison, J., Heath, W.R. & Carbone, F.R. Defective TCR expression in transgenic mice constructed using cDNA-based alpha- and beta-chain genes under the control of heterologous regulatory elements. *Immunol Cell Biol* **76**, 34-40 (1998).

58. Mombaerts, P. *et al.* RAG-1-deficient mice have no mature B and T lymphocytes. *Cell* **68**, 869-877 (1992).

59. Madisen, L. *et al.* A robust and high-throughput Cre reporting and characterization system for the whole mouse brain. *Nat Neurosci* **13**, 133-140 (2010).

60. Fonzi, W.A. & Irwin, M.Y. Isogenic strain construction and gene mapping in Candida albicans. *Genetics* **134**, 717-728 (1993).

61. Igyártó, B.Z. *et al.* Skin-resident murine dendritic cell subsets promote distinct and opposing antigen-specific T helper cell responses. *Immunity* **35**, 260-272 (2011).

62. Jaitin, D.A. *et al.* Massively parallel single-cell RNA-seq for marker-free decomposition of tissues into cell types. *Science* **343**, 776-779 (2014).

63. Kohen, R. *et al.* UTAP: User-friendly Transcriptome Analysis Pipeline. *BMC Bioinformatics* **20**, 154 (2019).

64. Moon, J.J. *et al.* Naive CD4(+) T cell frequency varies for different epitopes and predicts repertoire diversity and response magnitude. *Immunity* **27**, 203-213 (2007).

65. Pfaffl, M.W. A new mathematical model for relative quantification in real-time RT-PCR. *Nucleic Acids Res* **29**, e45 (2001).

Figure 1

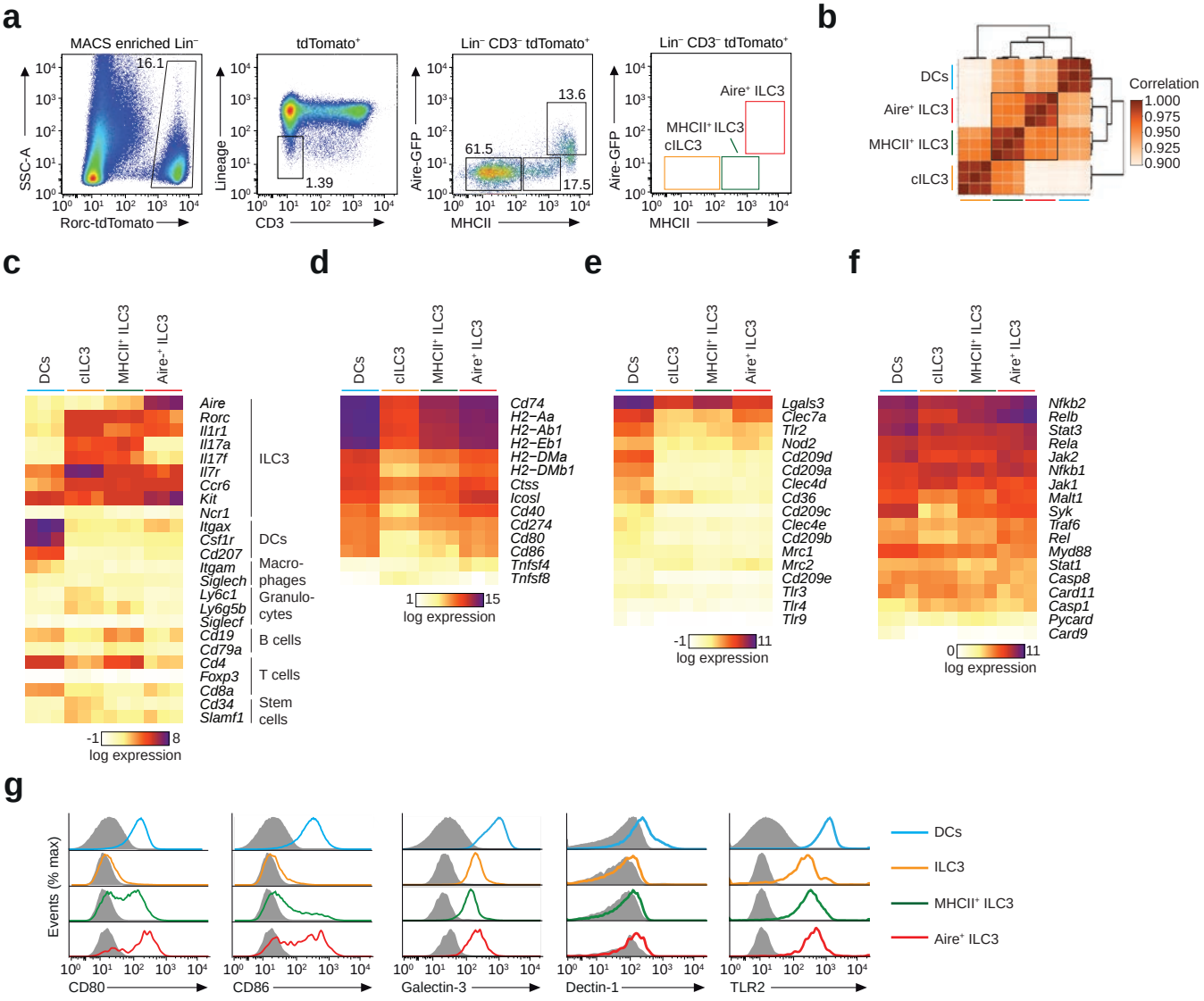
a
MACS enriched Lin⁻
16.1
SSC-A
Rorc-tdTomato
tdTomato⁺
Lineage
1.39
CD3
Lin⁻ CD3⁻ tdTomato⁺
13.6
61.5
17.5
Aire-GFP
MHCII
Aire⁺ ILC3
MHCII⁺ ILC3
cILC3
b
DCs
Aire⁺ ILC3
MHCII⁺ ILC3
cILC3
Correlation
1.000
0.975
0.950
0.925
0.900
c
DCs
cILC3
MHCII⁺ ILC3
Aire⁺ ILC3
Aire
Rorc
Il1r1
Il17a
Il17f
Il7r
Ccr6
Kit
Ncr1
ILC3
Itgax
Csf1r
Cd207
DCs
Itgam
Siglech
Macro-phages
Ly6c1
Ly6g5b
Siglecf
Granulo-cytes
Cd19
Cd79a
B cells
Cd4
Foxp3
Cd8a
T cells
Cd34
Slamf1
Stem cells
-1
8
log expression
d
Cd74
H2−Aa
H2−Ab1
H2−Eb1
H2−DMa
H2−DMb1
Ctss
Icosl
Cd40
Cd274
Cd80
Cd86
Tnfsf4
Tnfsf8
1
15
log expression
e
Lgals3
Clec7a
Tlr2
Nod2
Cd209d
Cd209a
Clec4d
Cd36
Cd209c
Clec4e
Cd209b
Mrc1
Mrc2
Cd209e
Tlr3
Tlr4
Tlr9
-1
11
log expression
f
Nfkb2
Relb
Stat3
Rela
Jak2
Nfkb1
Jak1
Malt1
Syk
Traf6
Rel
Myd88
Stat1
Casp8
Card11
Casp1
Pycard
Card9
0
11
log expression
g
Events (% max)
CD80
CD86
Galectin-3
Dectin-1
TLR2
DCs
ILC3
MHCII⁺ ILC3
Aire⁺ ILC3

Figure 2

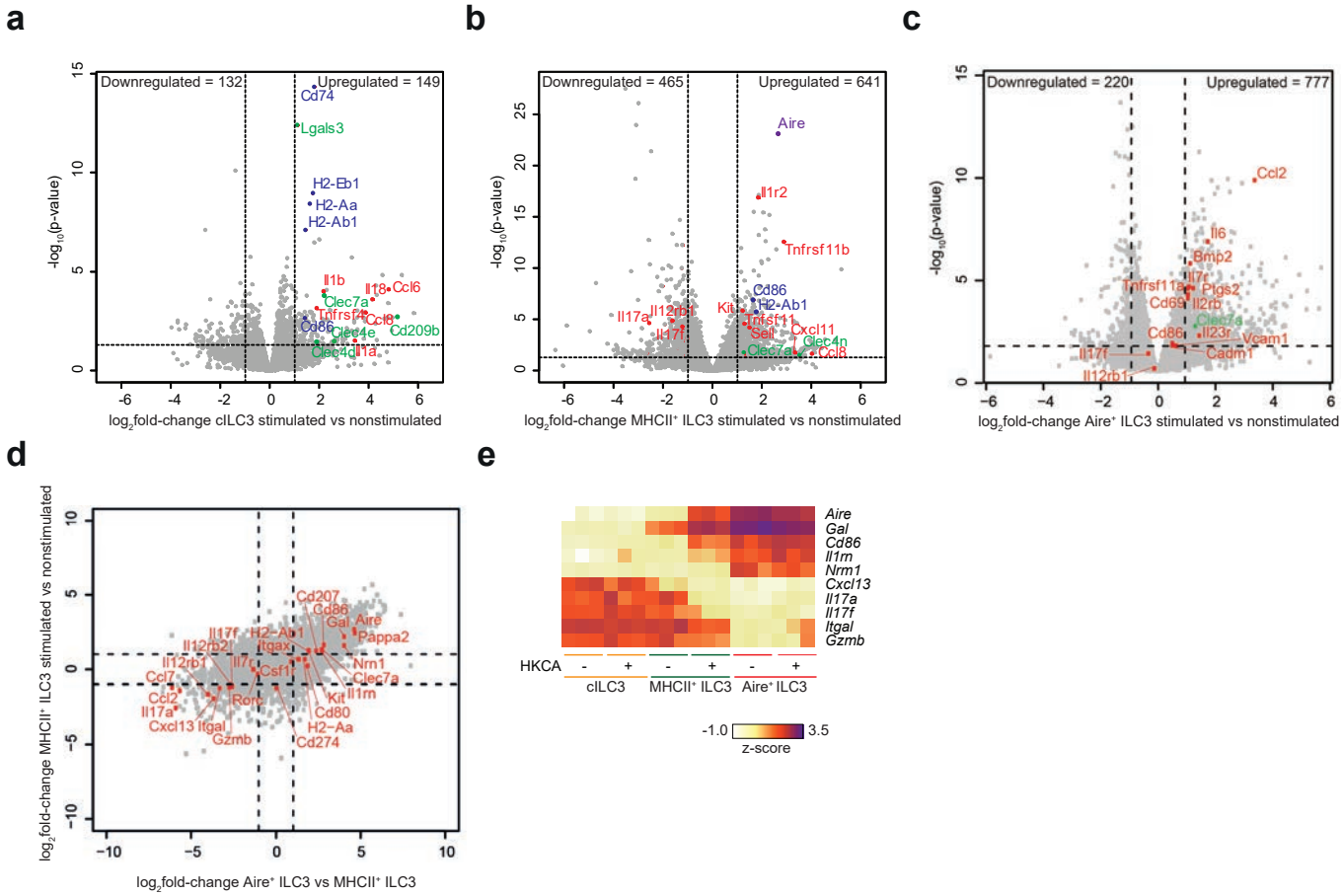
a
Downregulated = 132
Upregulated = 149
Cd74
Lgals3
H2-Eb1
H2-Aa
H2-Ab1
Il1b
Il18
Ccl6
Clec7a
Tnfrsf4
Ccl8
Cd86
Clec4e
Cd209b
Clec4d
Il1a
-log10(p-value)
log2fold-change cILC3 stimulated vs nonstimulated
b
Downregulated = 465
Upregulated = 641
Aire
Il1r2
Tnfrsf11b
Cd86
H2-Ab1
Il17a
Il12rb1
Il17f
Kit
Tnfrsf11
Sell
Cxcl11
Clec4n
Clec7a
Ccl8
-log10(p-value)
log2fold-change MHCII+ ILC3 stimulated vs nonstimulated
c
Downregulated = 220
Upregulated = 777
Ccl2
Il6
Bmp2
Il7r
Tnfrsf11a
Ptgs2
Cd69
Il2rb
Clec7a
Cd86
Il23r
Vcam1
Cadm1
Il17f
Il12rb1
-log10(p-value)
log2fold-change Aire+ ILC3 stimulated vs nonstimulated
d
Cd207
Cd86
Gal
Aire
Il17f
H2-Ab1
Pappa2
Il12rb2
Itgax
Il12rb1
Il7r
Csf1
Nrn1
Ccl7
Clec7a
Ccl2
Il1rn
Il17a
Rorc
Kit
Cd80
Cxcl13
Itgal
H2-Aa
Gzmb
Cd274
log2fold-change MHCII+ ILC3 stimulated vs nonstimulated
log2fold-change Aire+ ILC3 vs MHCII+ ILC3
e
Aire
Gal
Cd86
Il1rn
Nrm1
Cxcl13
Il17a
Il17f
Itgal
Gzmb
HKCA
-
+
-
+
-
+
cILC3
MHCII+ ILC3
Aire+ ILC3
-1.0
3.5
z-score

Figure 3

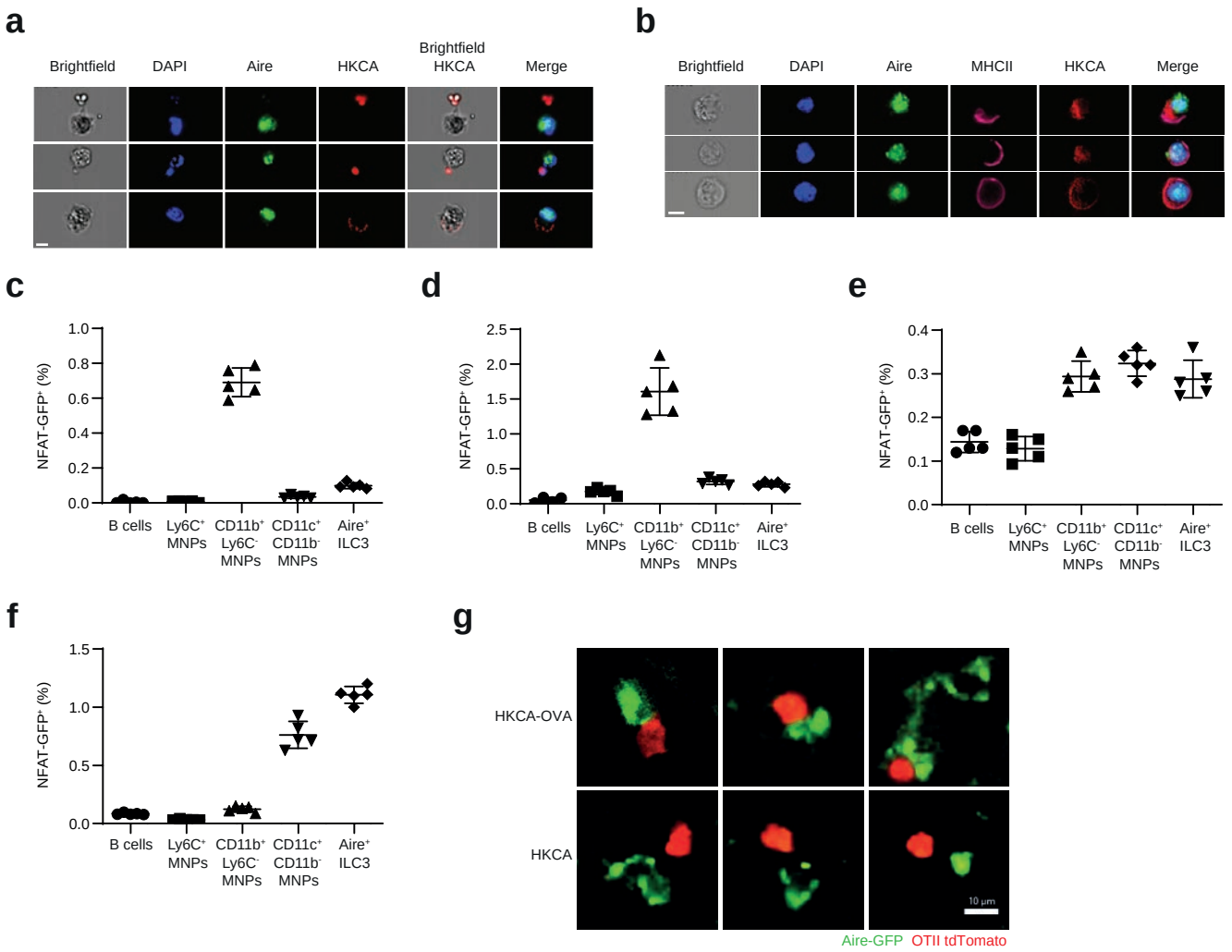
a
Brightfield
DAPI
Aire
HKCA
Brightfield HKCA
Merge
b
Brightfield
DAPI
Aire
MHCII
HKCA
Merge
c
NFAT-GFP+ (%)
1.0
0.8
0.6
0.4
0.2
0.0
B cells
Ly6C+ MNPs
CD11b+ Ly6C- MNPs
CD11c+ CD11b- MNPs
Aire+ ILC3
d
NFAT-GFP+ (%)
2.5
2.0
1.5
1.0
0.5
0.0
B cells
Ly6C+ MNPs
CD11b+ Ly6C- MNPs
CD11c+ CD11b- MNPs
Aire+ ILC3
e
NFAT-GFP+ (%)
0.4
0.3
0.2
0.1
0.0
B cells
Ly6C+ MNPs
CD11b+ Ly6C- MNPs
CD11c+ CD11b- MNPs
Aire+ ILC3
f
NFAT-GFP+ (%)
1.5
1.0
0.5
0.0
B cells
Ly6C+ MNPs
CD11b+ Ly6C- MNPs
CD11c+ CD11b- MNPs
Aire+ ILC3
g
HKCA-OVA
HKCA
10 µm
Aire-GFP OTII tdTomato

Figure 4

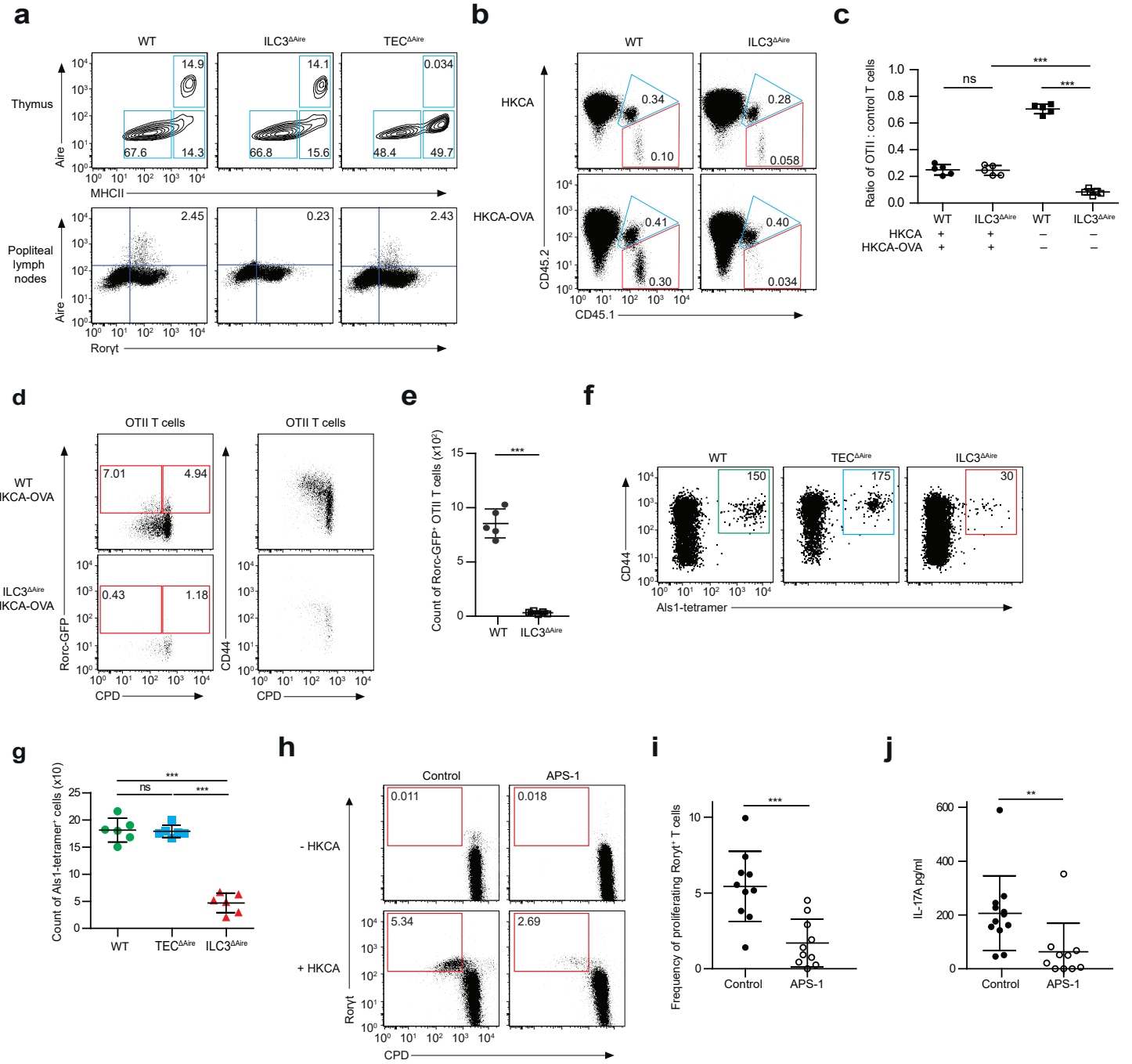
a
WT
ILC3ΔAire
TECΔAire
Thymus
Aire
MHCII
14.9
67.6
14.3
14.1
66.8
15.6
0.034
48.4
49.7
Popliteal lymph nodes
Roryt
2.45
0.23
2.43
b
HKCA
HKCA-OVA
CD45.2
CD45.1
0.34
0.10
0.28
0.058
0.41
0.30
0.40
0.034
c
Ratio of OTII : control T cells
ns
***
HKCA
HKCA-OVA
d
OTII T cells
WT HKCA-OVA
ILC3ΔAire HKCA-OVA
Rorc-GFP
CD44
CPD
7.01
4.94
0.43
1.18
e
Count of Rorc-GFP+ OTII T cells (x10²)
f
Als1-tetramer
150
175
30
g
Count of Als1-tetramer+ cells (x10)
h
Control
APS-1
- HKCA
+ HKCA
0.011
0.018
5.34
2.69
i
Frequency of proliferating Roryt+ T cells
j
IL-17A pg/ml
**

Figure 5

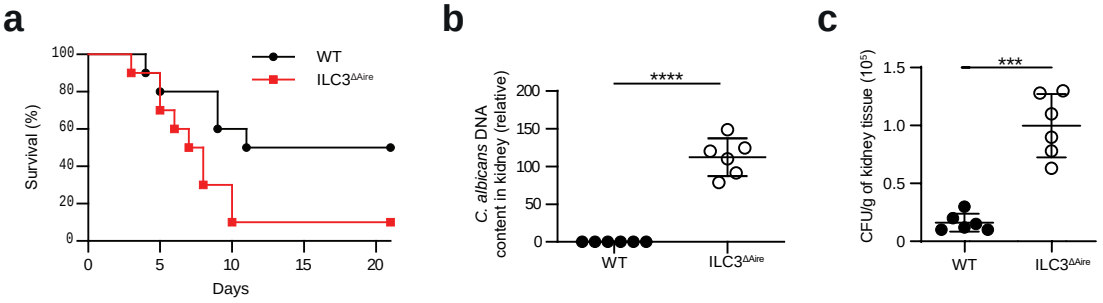
a
Survival (%)
100
80
60
40
20
0
0
5
10
15
20
Days
WT
ILC3ΔAire
b
C. albicans DNA content in kidney (relative)
200
150
100
50
0
****
WT
ILC3ΔAire
c
CFU/g of kidney tissue (10⁵)
1.5
1.0
0.5
0
***
WT
ILC3ΔAire

Figure 6

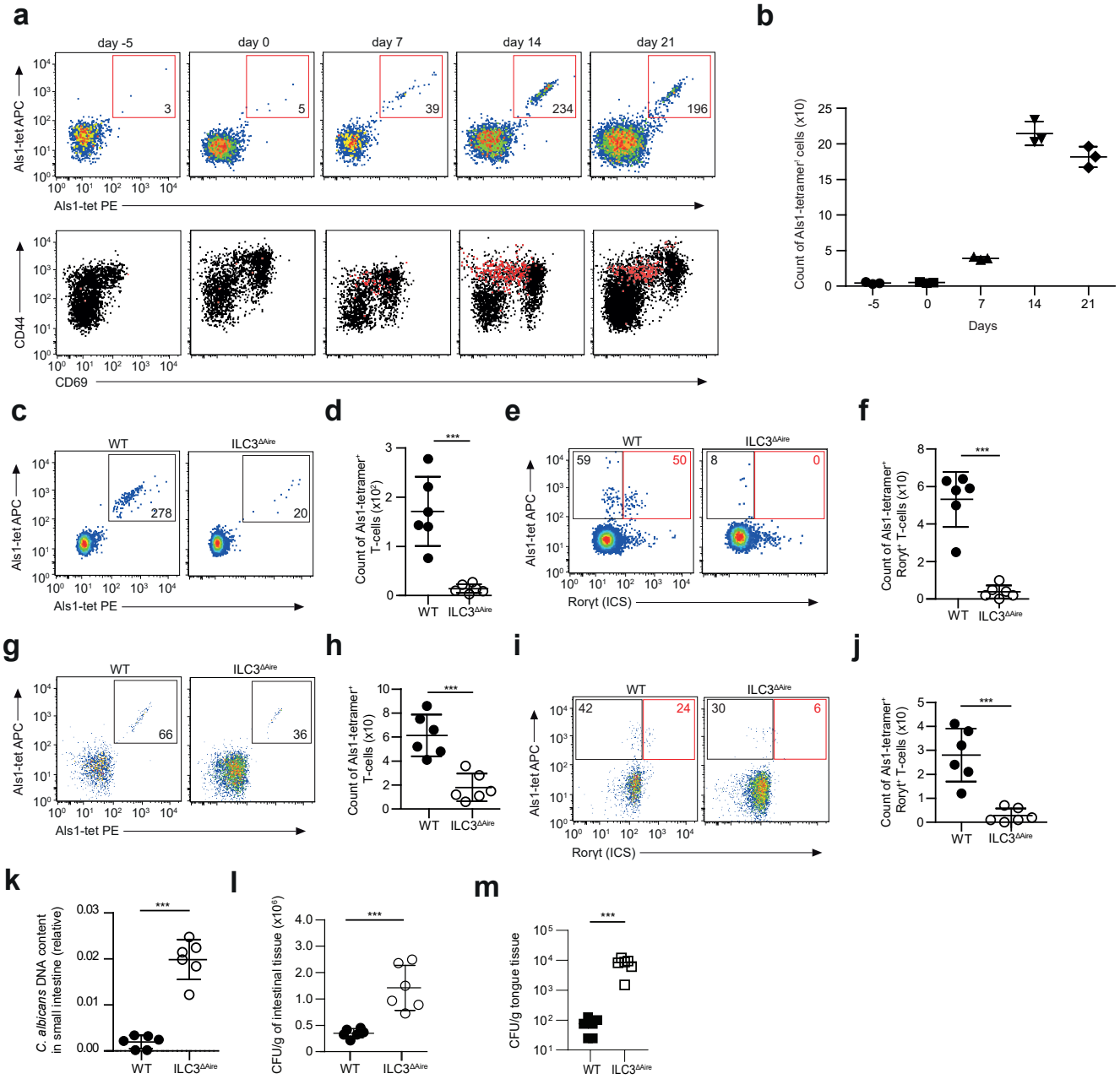
a
day -5
day 0
day 7
day 14
day 21
3
5
39
234
196
Als1-tet APC
Als1-tet PE
CD44
CD69
b
Count of Als1-tetramer+ cells (x10)
Days
c
WT
ILC3ΔAire
278
20
d
Count of Als1-tetramer+ T-cells (x10²)
***
e
59
50
8
0
Rorγt (ICS)
f
Count of Als1-tetramer+ Rorγt+ T-cells (x10)
g
66
36
h
Count of Als1-tetramer+ T-cells (x10)
i
42
24
30
6
j
Count of Als1-tetramer+ Rorγt+ T-cells (x10)
k
C. albicans DNA content in small intestine (relative)
l
CFU/g of intestinal tissue (x10⁶)
m
CFU/g tongue tissue

Figure 7

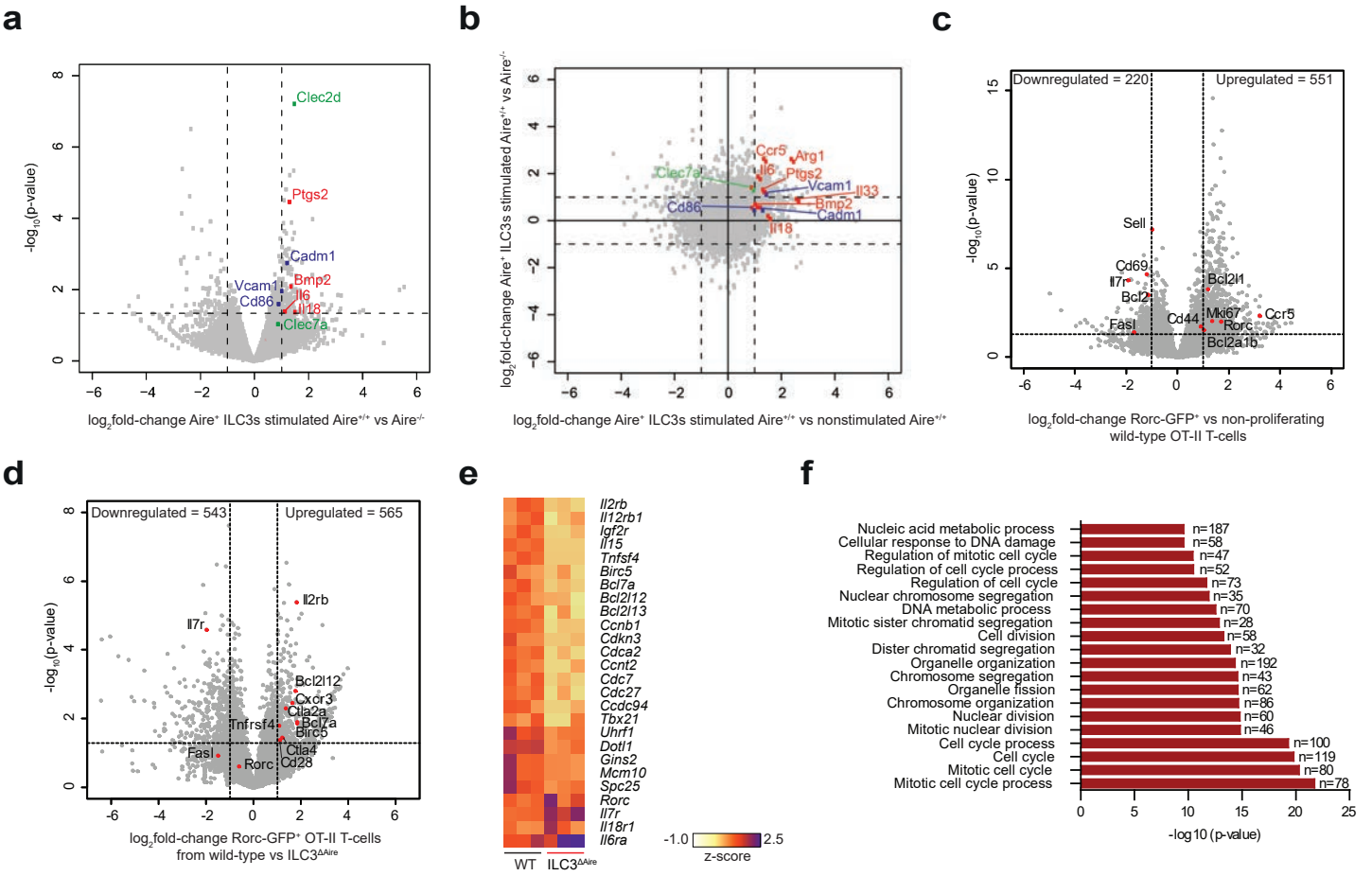
a
Clec2d
Ptgs2
Cadm1
Vcam1
Bmp2
Cd86
Il6
Il18
Clec7a
-log10(p-value)
log2fold-change Aire+ ILC3s stimulated Aire+/+ vs Aire-/-
b
Ccr5
Arg1
Il6
Ptgs2
Vcam1
Il33
Clec7a
Cd86
Bmp2
Cadm1
Il18
log2fold-change Aire+ ILC3s stimulated Aire+/+ vs Aire-/- ILC3s stimulated Aire+/+ vs nonstimulated Aire+/+
c
Downregulated = 220
Upregulated = 551
Sell
Cd69
Il7r
Bcl2
Fasl
Cd44
Bcl2l1
Mki67
Rorc
Ccr5
Bcl2a1b
-log10(p-value)
log2fold-change Rorc-GFP+ vs non-proliferating wild-type OT-II T-cells
d
Downregulated = 543
Upregulated = 565
Il2rb
Il7r
Bcl2l12
Cxcr3
Ctla2a
Tnfrsf4
Bcl7a
Birc6
Ctla4
Cd28
Fasl
Rorc
-log10(p-value)
log2fold-change Rorc-GFP+ OT-II T-cells from wild-type vs ILC3ΔAire
e
Il2rb
Il12rb1
Igf2r
Il15
Tnfsf4
Birc5
Bcl7a
Bcl2l12
Bcl2l13
Ccnb1
Cdkn3
Cdca2
Ccnt2
Cdc7
Cdc27
Ccdc94
Tbx21
Uhrf1
Dotl1
Gins2
Mcm10
Spc25
Rorc
Il7r
Il18r1
Il6ra
WT
ILC3ΔAire
-1.0
2.5
z-score
f
Nucleic acid metabolic process n=187
Cellular response to DNA damage n=58
Regulation of mitotic cell cycle n=47
Regulation of cell cycle process n=52
Regulation of cell cycle n=73
Nuclear chromosome segregation n=35
DNA metabolic process n=70
Mitotic sister chromatid segregation n=28
Cell division n=58
Dister chromatid segregation n=32
Organelle organization n=192
Chromosome segregation n=43
Organelle fission n=62
Chromosome organization n=86
Nuclear division n=60
Mitotic nuclear division n=46
Cell cycle process n=100
Cell cycle n=119
Mitotic cell cycle n=80
Mitotic cell cycle process n=78
-log10 (p-value)

Extended Data Figure 1 (related to Figure 2A-C)

a

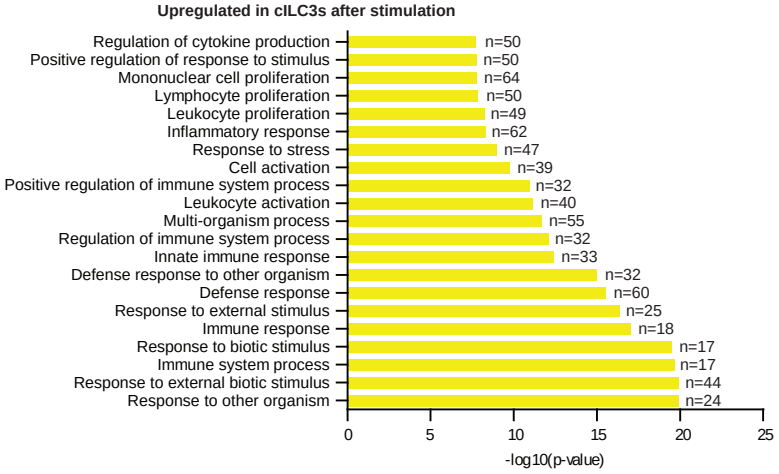

b

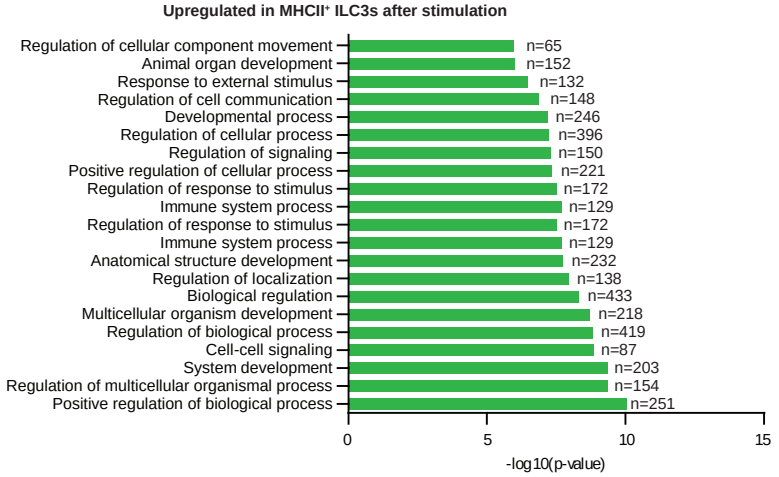

c

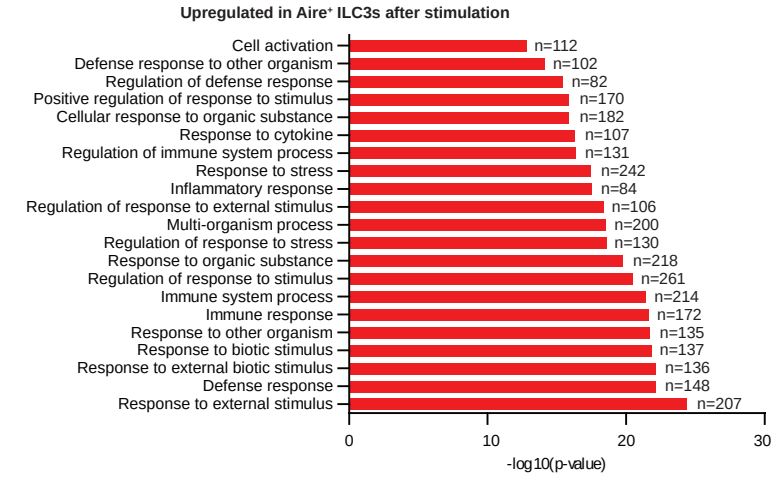

d

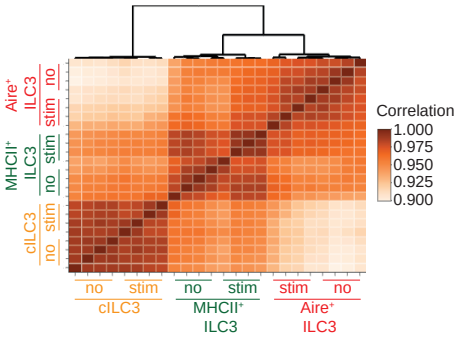

Extended Data Figure 2 (related to Figure 3)

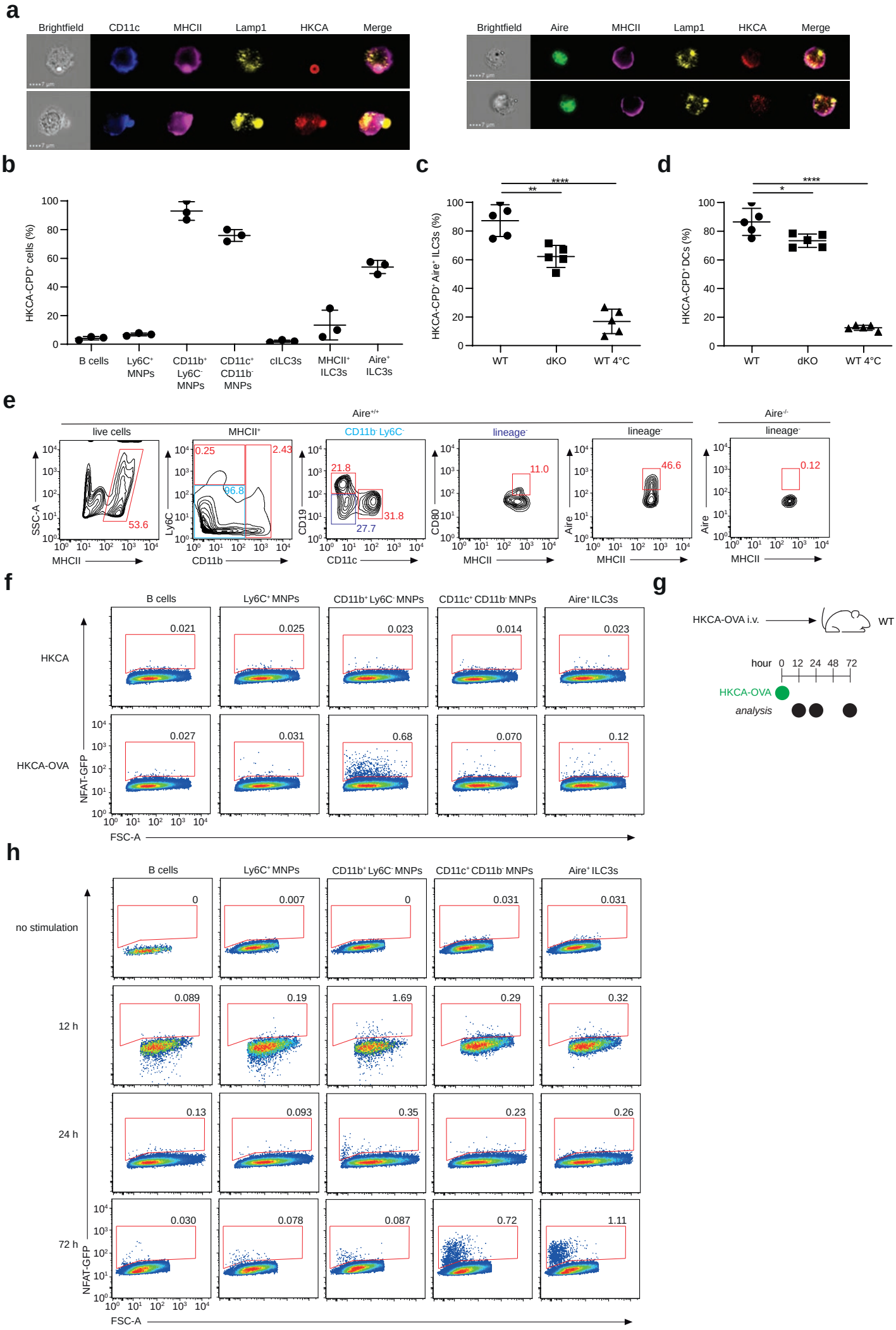

Extended Data Figure 3 (related to Figure 4 and 5)

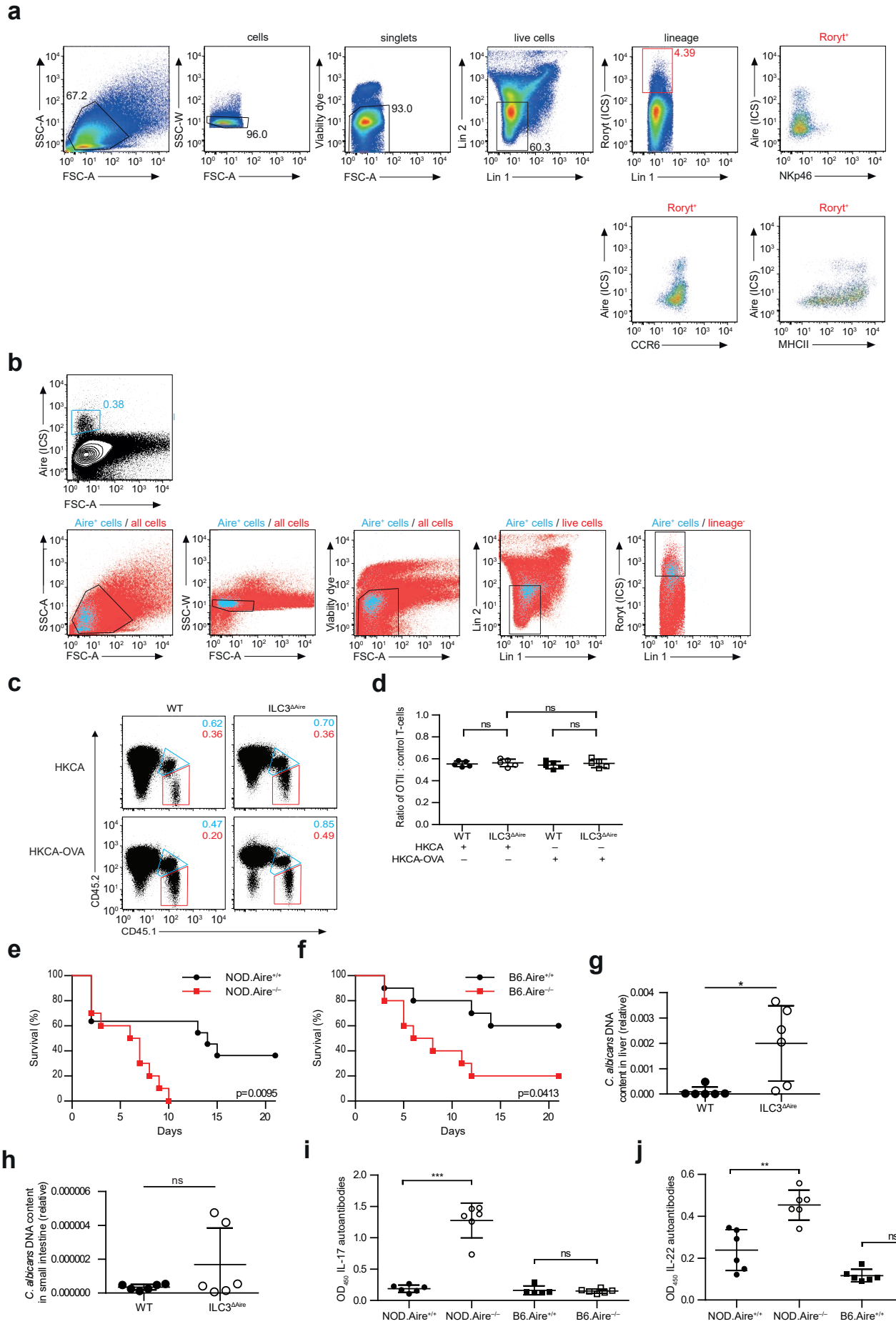

Extended Data Figure 4 (related to Figure 6)

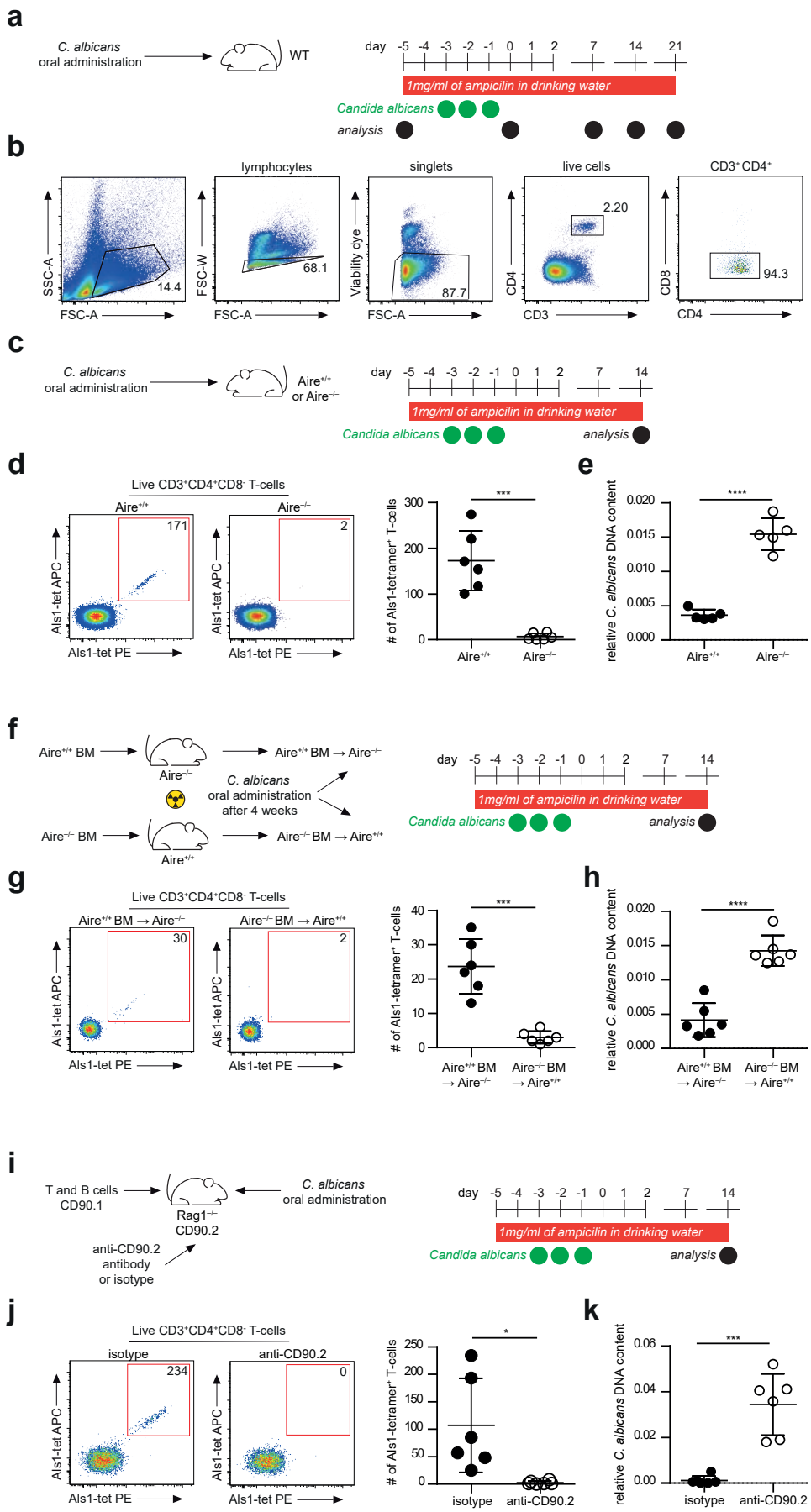

Extended Data Figure 5 (related to Figure 6)

a

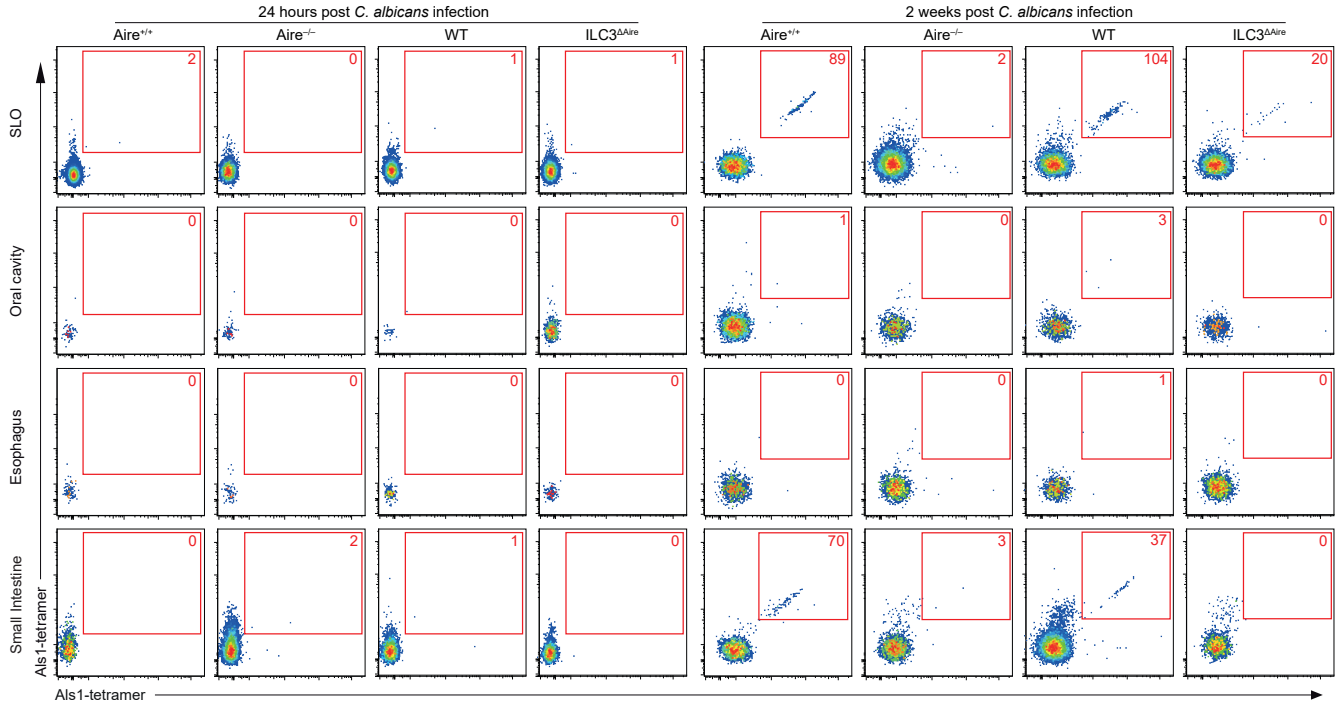

b

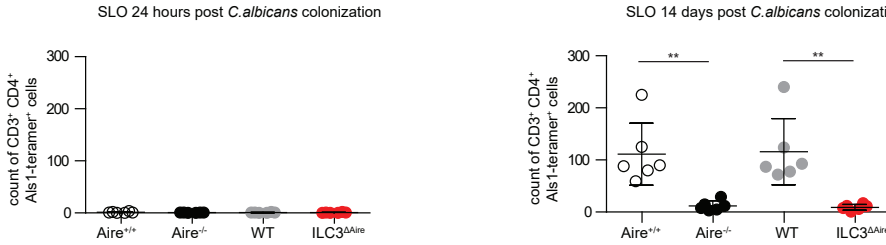

c

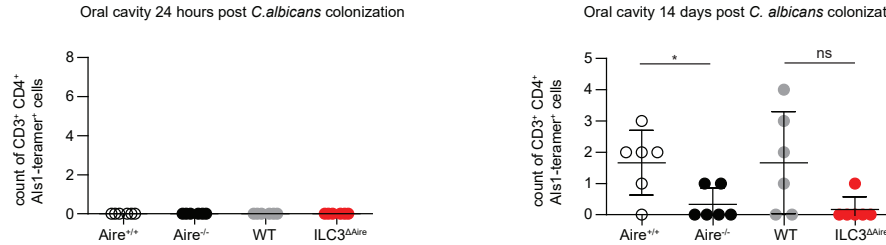

d

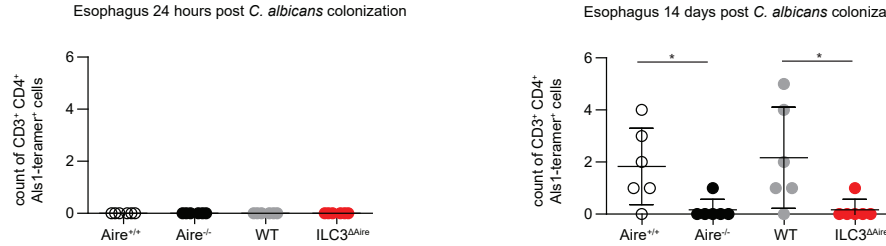

e

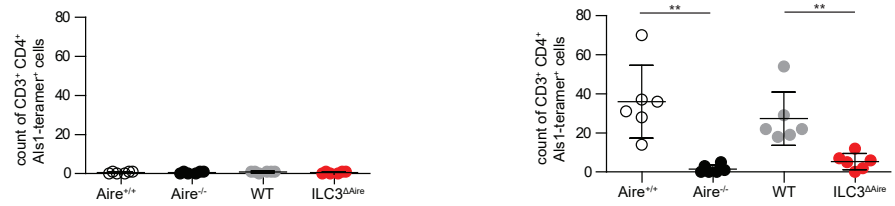

Extended Data Figure 6 (related to Figure 6)

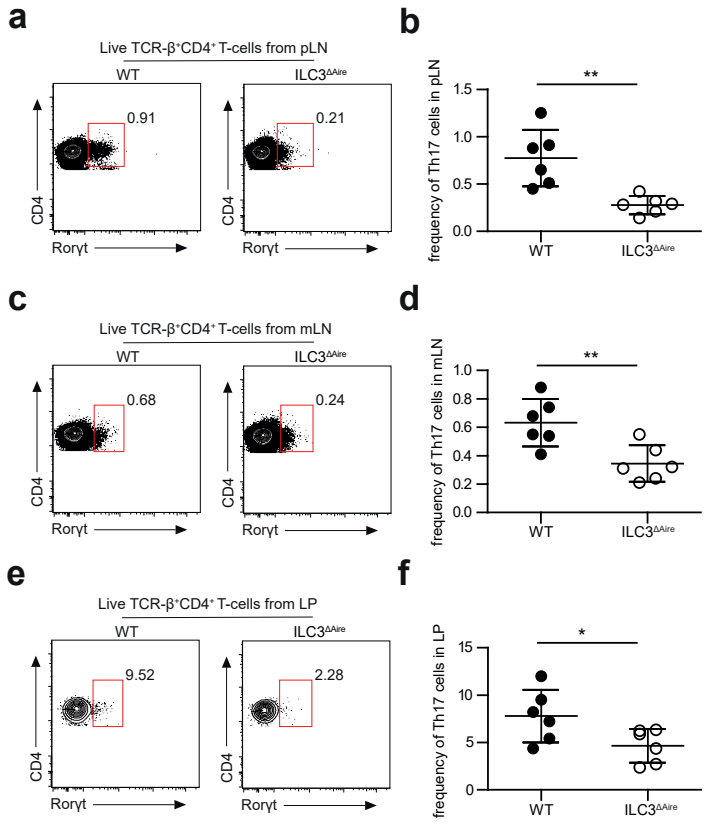

Extended Data Figure 7 (related to Figure 6)

a

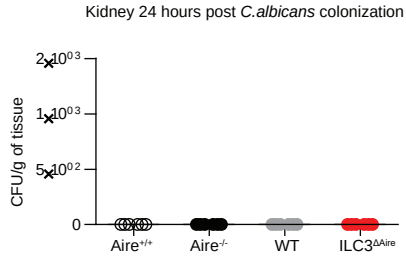

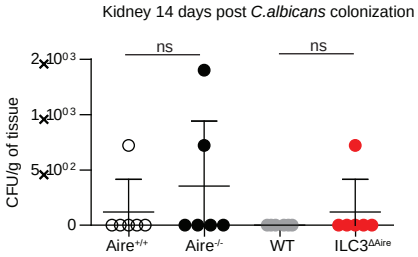

b

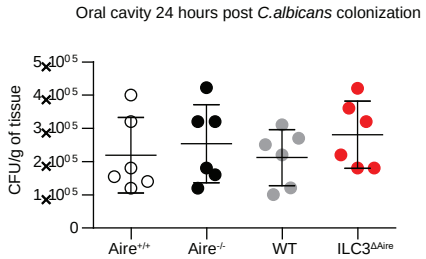

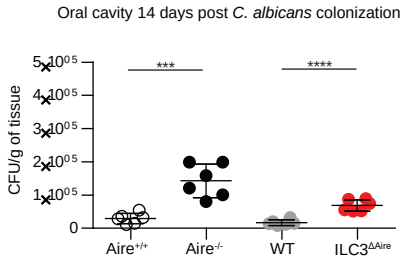

c

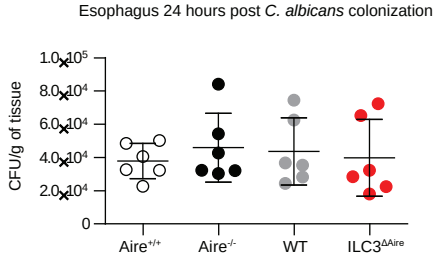

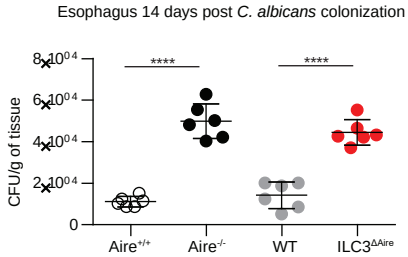

d

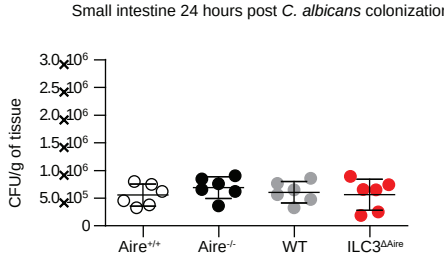

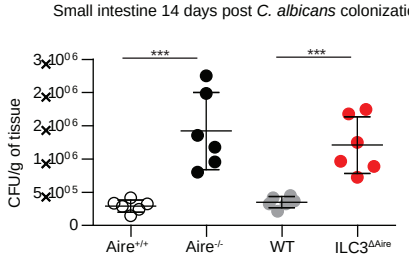

Extended Data Figure 8

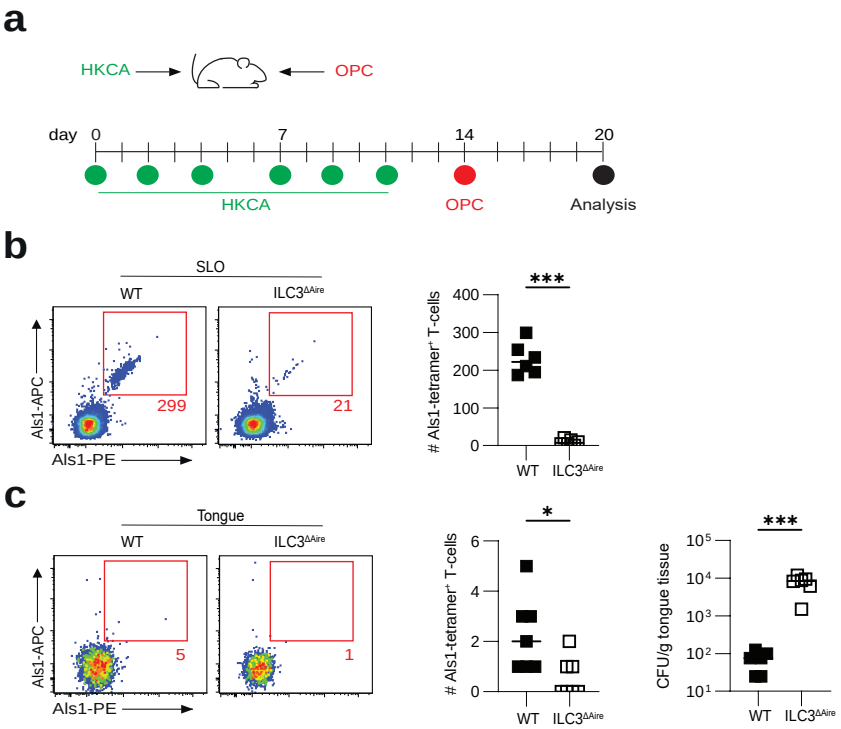

Extended Data Figure 9 (related to Figure 7A-B)

a

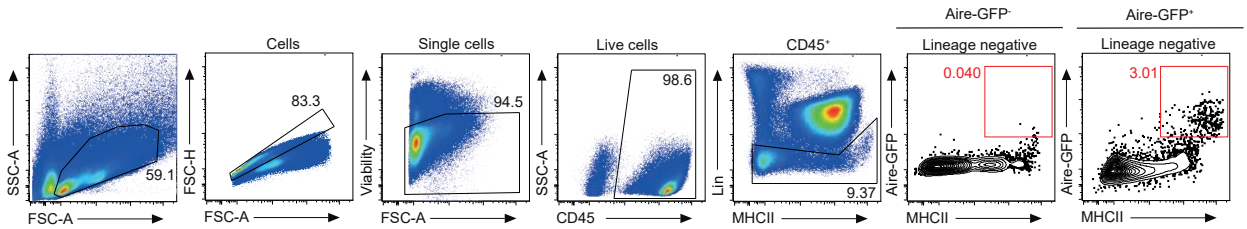

b

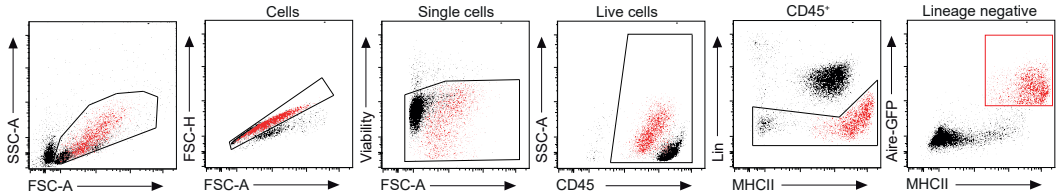

Extended Data Figure 10 (related to Figure 7C, D)

a

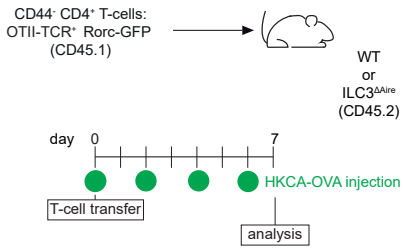

b

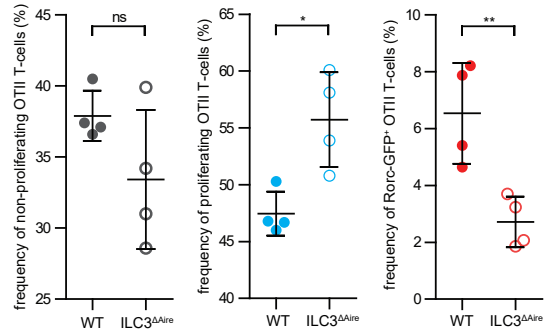

c

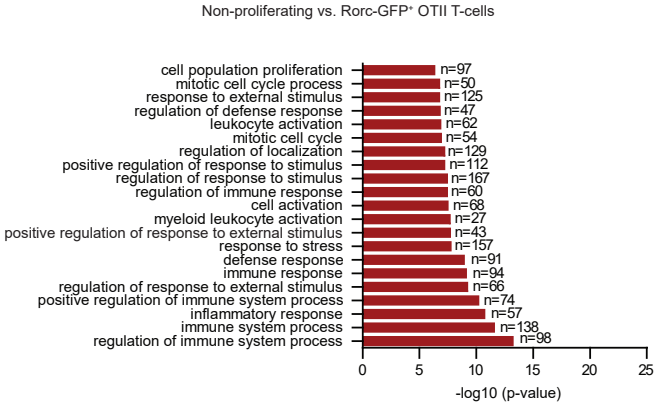

d

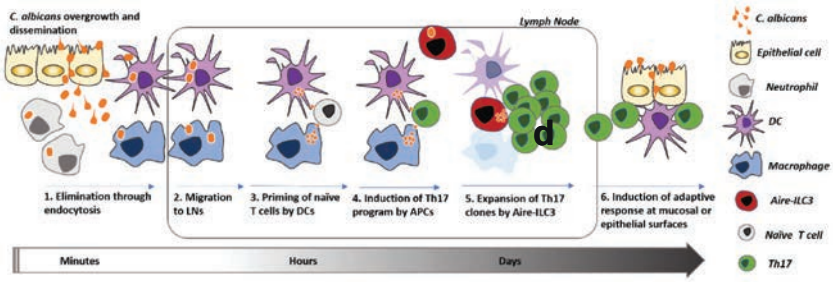

e